Incineration of Aviary Manure: the Case Studies of Poultry Litter and Laying Hens Manure

Ario Fahimi, Elza Bontempi, Laura Fiameni, Alexandra Guedes, Renato Guimarães, Karen Moreira, Ana Cláudia Santos, Bruno Valentim, Georgeta Predeanu, Mihaela Bălănescu, et al.

Incineration of Aviary Manure: the Case Studies of Poultry Litter and Laying Hens Manure

Ario Fahimi [1,*], Elza Bontempi [1], Laura Fiameni [1], Alexandra Guedes [2], Renato Guimarães [2], Karen Moreira [2], Ana Cláudia Santos [2], Bruno Valentim [2], Georgeta Predeanu [3], Mihaela Bălănescu [3] Hayati Olgun [4], Marie Christine Boiron [5] and Michel Cathelineau [5]

[1] INSTM and Chemistry for Technologies Laboratory, Department of Mechanical and Industrial Engineering, University of Brescia, via Branze, 38, 25123, Brescia, Italy; a.fahimi@unibs.it (A.F.); elza.bontempi@unibs.it (E.B.); l.fiameni001@unibs.it (L.F.)

[2] Earth Science Institute – Porto pole, Department of Geosciences, Environment and Spatial Plannings, Faculty of Sciences, University of Porto, rua do Campo Alegre s/n, 4169 – 007 Porto, Portugal; aguedes@fc.up.pt (A.G.); up200506169@edu.fc.up.pt (R.G.); karen.moreira@fc.up.pt (K.M.); anasantos@fc.up.pt (A.C.S.); bvvalent@fc.up.pt (B.V.)

[3] University Politehnica of Bucharest, Faculty of Applied Chemistry and Materials Science, Research Center for Environmental Protection and Eco-friendly Technologies, 1, Polizu St., 011061, Bucharest, Romania; gpredeanu@gmail.com (G.P.); mihaela.balanescu@beia.ro (M.B.)

[4] Ege Üniversitesi Güneş Enerjisi Enstitüsü, 119/1, sokak 2, Bornova, Izmir 35100, Turkey; hayati.olgun@ege.edu.tr (H.O.)

[5] Université de Lorraine, CNRS, CREGU, GeoRessources Lab., Campus Aiguillettes, Faculté des Sciences et Technologies, rue Jacques Callot, Vandoeuvre-lès-Nancy F-54506, France; marie-christine.boiron@univ-lorraine.fr (M.C.B.); michel.cathelineau@univ-lorraine.fr (M.C.);

***** Corresponding author: a.fahimi@unibs.it (A.F.)

Abstract

The industrial incineration of aviary manure is still far from the concept of using its ash residuals for nutrient uptake by plants, and most of these materials are landfilled under futile fixed cost. Aviary manure includes poultry litter mixed with different aviary bedding materials or laying hens manure, which may be burned using other incineration technologies and conditions. This study aims to determine the comparative characterisation of P-rich ash residues sampled at Güres Energy (Turkey) fluidised bed combustion of laying hens manure and at Campoaves (Portugal)

chain grate stoker combustion of rice husk poultry litter. The effect of different fuels and different combustion systems on P speciation in ash was investigated: the characterisation of global samples (bottom ash (BA), economiser fly ash (FAECO), cyclone fly ash (FACYC)) and respective size-fractions were done chemically (proximate and elemental analysis by X-ray fluorescence – XRF – and Inductively Coupled Plasma Mass Spectroscopy – ICP-MS), morphologically (detailed imaging and X-ray microanalysis by Scanning Electron Microscopy–Energy-Dispersive X-ray spectrometry – SEM–EDS) and mineralogically (X-ray diffraction – XRD). Phosphorus was detected in Güres ashes mainly as hydroxyapatite crystals alongside $CaCO_3$ relics and CaO. At the same time, Campoaves ash fractions contained P also as Na-K-Mg phosphate and significant amounts of rice husk relics, including unburnt char and silica phases. Both Güres and Campoaves ashes are complex, but the combustion of aviary manure under these setting conditions appears to be promising for P recovery owing to their high P content and limited trace elements respecting the limitations of EU legislation for fertilisers applications.

Graphical abstract

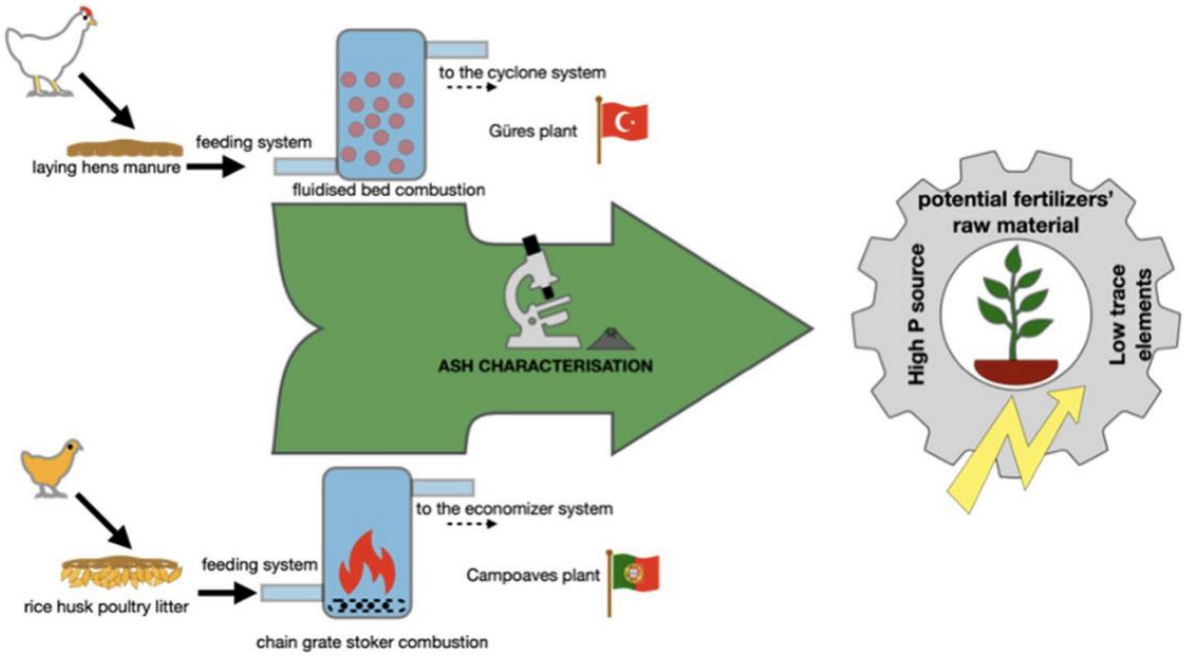

Statement of novelty

This paper compares two sub-categories of incinerated aviary manure (rice husk poultry litter ash and laying hens manure ash) under two different combustion systems (fluidised bed gasifier and chain grate stoker) in terms of chemical, mineralogical and morphological characterisation. The novelty lies in studying the effect of fuel and combustion systems on the P speciation and possible use in the fertiliser industry. The results showed the trace element contents in acid leachate comply with EU fertilisers regulations: this paves the way for future study about plant availability tests and eventual direct application in agriculture as fertilisers.

Keywords

Phosphorus; Incineration; Ash; Characterisation; Aviary manure; Sustainability

Introduction

Phosphorus is a vital micronutrient, mostly occurring as phosphate (PO_4^{3-}), for food and crop production that is mainly obtained from phosphate rocks mining, from which P-bearing minerals (e.g. apatite) are concentrated and then processed to obtain fertilisers [1].

The demand for P-based fertilisers is expected to double by 2050 due to population growth [2]. Still, the concentration of phosphate rock deposits in a few countries and markets instability and uncertainty could lead to eventual spikes in the market price affecting the fertilisers industry, which covers up to 80 % of the market related to P [3, 4]. This situation led the European Commission to include phosphate rocks on the list of the 20 most critical raw materials to stimulate proper management of the resource from farmers, agricultural industries and policymakers, and P-recycling [5].

On the other hand, it has to be considered that only less than 20 % of the P used in the food and feed production sectors are anthropogenically consumed [6]. Meaning that we must focus on the significant losses (primarily associated with meat production and crop farming [7]). Among the principal waste streams, animal manure represents the most important secondary source of P in order of importance under the European Commission [8,9].

In particular, aviary manure (e.g. poultry litter and laying hens manure) is a promising secondary source of P [10] since one-third of the P is digested during the bird life cycle, and the remaining P is excreted in manure [11]. Additionally, the amount of manure being produced will increase since poultry meat production alone already covers approximately 35% of global meat production, owing to an increase of more than 12 fold over the last 50 years [12]. In the past, farmers already used aviary manure as a substitute for chemical fertilisers in croplands and soil amendments [12–14]. Still, it has been exclusively applied to the local farms due to its high density/volume ratio leading to the high cost of transportation to incinerators [15].

The manure composition is variable and is based on the type of housing system, diet and manure handling (e.g., bedding material, storage, reuse frequency). However, apart from P, it also contains other plant macronutrients such as N and K, which together seem readily plant available. However, the latter may cause plant stress (also known as plant burning) due to their excessive concentration in the soil [16, 17]. Alongside it, there are issues related to the presence of pathogenic microorganisms, ammonia emissions and the eventual eutrophication of surface and ground waterways via nutrient runoff [6, 13, 18–21] that could jeopardise the environment: specific limits about nutrient contents in are set in waste streams to preserve a proper ecological condition (e.g., Sewage Sludge Directive 86/278/ECC, Water Framework Directive 2000/60/EC, Nitrates Directive 91/676/EEC) [6].

The incineration of poultry manure effectively reduces the waste volume to alleviate the disposal problem, avoids the leaching of nutrients, eliminate pathogens and toxic organic substances, and evaporate nitrogen. The P-rich ash residue may be usable as a possible substitute of phosphate rock for the production of fertilisers with a low concentration of rare earth elements [2, 21].

The incineration of poultry litter on farms has been incentivised across the EU since 2014 to produce green energy with the economic advantage of a shorter pay-back period [19][22]. However, there were some drawbacks due to using a high moisture fuel with low energy value, variable chemical composition with increased contents of S, N and Cl – being considered in the category of agricultural biomass [23] – which can lead to metal corrosion. Finally, high ash content may lead to deposit formation such as slagging and fouling due to the low-temperature melting materials formed under the presence of elements such as Si, K [19, 21]. In addition, aviary manure ash has been impeached by legal limits regarding elements such as Cu and Zn [2]. Thus, as a consequence, despite its qualities as an organic fertiliser and P-Ca source in poultry feeds [24], it is treated as a residue and not as a by-product and is usually landfilled [25].

Considering the lack of information regarding solutions for aviary manure ash, it seems pertinent to promote aviary manure ash for different possible applications. The characterisation of different types of aviary manure ash in terms of elemental and mineral composition for the description of P speciation has been thus undertaken. Leaching tests were used then to estimate the P extractability of the final potential for nutrient reuse [26].

However, it would be essential to explain the broad P chemical speciation after undergoing different thermal reactions to form dissolved salts and mineralised materials (e.g., hydroxyapatite). Following this perspective, developing strategies for recovering and valorising P (as critical raw material to be kept in the value chain) represents a pillar in managing agricultural waste within a circular economy [20].

Therefore, this research aims to identify the ash specificities depending on the aviary manure, incineration technologies and sampling locations. For this purpose, detailed characterisation by a combination of multiple techniques was carried on aviary ash from two different sub-categories of aviary production after the combustion: ash from the chain grate stoker incineration of rice husk poultry litter and, and ash from fluidised bed combustion of laying hens manure.

Materials and Methods

Sampling location

The fuel and ash samples were collected at the incinerators of Campoaves (Figueira da Foz, Portugal; hereinafter referred to as “CA”) and Güres Energy (Manisa, Turkey; referred to as “GU”). These two incinerators show fundamental concept differences between them regarding the fuels and the combustion technologies. The two produced ash types consequently pose contrasted challenges for P-recovery and the utilisation of residues after P-recovering:

(i) at Campoaves (CA), the manure is a rice husk poultry litter (referred to as “RHPL”) composed of poultry excreta mixed with the rice husks used as aviary bedding from the surrounding rice fields. The fuel, however, is composed of woodchips and RHPL. These components may be in the form of thick crusts (5-10 cm) of rice husk (RH) cemented by poultry excreta formed in the aviary bedding top layers and as loose RH with some faeces from the deepest layers of the aviary bedding. Before incineration, the RHPL is pre-dried, and its

combustion is then made together with large (approx. 5 cm) woodchips in a chain grain stoker for several minutes and a temperature set to reach 1000 °C to comply with the directive 2000/76/EC [27] aimed for the removal of pathogens (Fig. 1A).

(ii) At Güres (GU), where eggs are produced, the manure is coming from laying hens kept in cages (no bedding) and composed of a mixture of excreta, broken eggshells and feathers (laying hens manure, referred to as "LHM"). At Güres Energy, the manure is dried, and the moisture is reduced to 20 wt. %. Before combustion, the LHM mixed with biomass is firstly gasified and then burnt, for ca. 2 s at 850-950 °C, inside a fluidised bed reactor. In the combustion chamber, quartz (SiO_2) sand is initially used as a solid heat carrier for furnace heat distribution, and then calcite ($CaCO_3$) sand is used for sulfur capture (Fig. 1B).

Samples

At Campoaves, the raw RHPL was randomly sampled directly from different parts and depths of the pile using a plastic shovel and then mixed to ensure the sampling representability. Specific portions of droppings crusts and loose poultry litter were also collected to obtain rich and poor droppings fractions. All samples were immediately stored in thick plastic bags and analysed on that same day.

Simultaneously, global ash samples from three different spots were also collected: bottom ash (BA) directly from the exit of the water tank; economiser fly ash (FAECO) from the economiser ash hopper adjoining the combustion chamber; cyclone fly ash (FACYC) from the multi-cyclone hopper. The samples were stored in thick plastic bags and were oven-dried at 50 °C the same day until reaching a constant weight. Manually, they were split through the coning method after getting 100 g samples using a riffling splitter. Finally, one of the 100 g sub-samples was divided into 12.5 g sub-samples via a rotary sample divisor combined with a vibratory feeder (Retsch PT 100 + DR 100, Hann, Germany) [28]. Workers at Güres Group sampled fresh and undried LHM after being conveyed from the laying hens building. BA, FACYC and FAECO samples were collected from the respective hoppers and dried and sorted as mentioned for Campoaves samples.

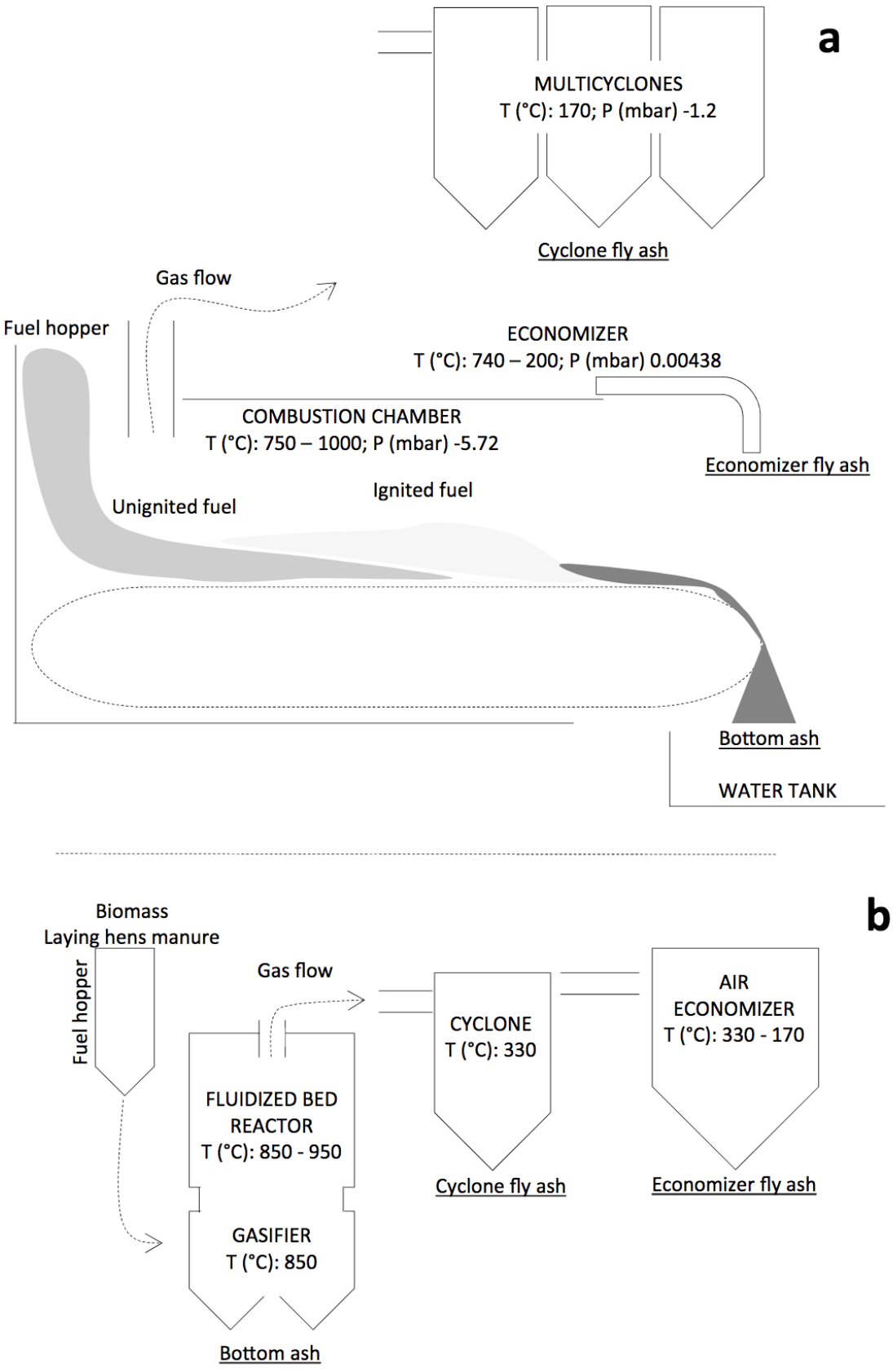

175

176 Figure 1. Schematic process diagram of the combustion systems: A) Chain grate stoker at
177 "Campoaves" (Figueira da Foz, Portugal); B) Gasifier and fluidised bed reactor at "Güres Energy"
178 (Izmir, Turkey).

Size-determination via sieving

The RHPL sampled from Campoaves (crusts not included) was manually sieved using 5 and 10 mesh sieves (4 mm and 2 mm, respectively). Different size fractions were obtained from the global ash samples of Güres. For this purpose, dry sieving was carried using a sieve agitator (Retsch AS200, Hann, Germany) in 2 rounds of 10 min agitation at 70% vibration amplitude (as an adaptation according to DS/EN 15149-2 [29]), and a column of sieves of 150 µm, 75 µm, 45 µm and 25 µm for FACYC and FAECO sample, while for BA sample a different column of sieves was used: 4 mm, 2 mm, 1 mm, 0.5 mm, 250 µm, 125 µm and 63 µm. Size-fractions were not obtained from Campoaves ashes due to particles agglomeration generating false coarse particles and reducing the amount and type of fine particles.

Proximate and elemental analysis and loss on ignition (LOI)

The proximate analyses were made for both Campoaves and Güres (here also for the different size fractions) samples to determine moisture, volatile matter, ash, and the fixed carbon calculation. For each test, 1 g ± 0.1 of samples was weighed on a laboratory balance (Sartorius Analytic, Göttingen, Germany), and all global ash samples and the size-fraction samples >75 µm were grounded with a mortar to pass the 200 mesh (75 µm) sieve. The moisture content was measured in compliance with ISO 11722 [30]. The samples were oven-heated at 105 °C until reaching a constant weight in a Carbolite Furnace with nitrogen flow and then cooled in a desiccator to reach room temperature (25 °C) and weighed. The ash and volatile matter content were measured according to ISO 1171 [31] and ISO 562 [32]. For the ash determination, the samples were heated inside crucibles at 815 °C until reaching a constant weight in a muffle furnace (47900-Thermolyne). After that, the ash was cooled in a desiccator to reach room temperature (25 °C) and weighed. The samples were heated inside crucibles at 900 °C for 7 minutes in a muffle furnace to determine the volatile matter (47900-Thermolyne). After that, the ash was cooled in a desiccator and weighed.
Major oxides, Loss on Ignition (LOI) and total C and S were determined at Bureau Veritas Commodities Canada Ltd. (Vancouver, Canada). Major oxides were determined by X-Ray Fluorescence (XRF) after samples fusion with lithium tetraborate/metaborate and casting into glass discs, and LOI was determined at 1000 °C.

Total Phosphorus determination, minor and trace elements

Spectrophotometry measurements for the quantification of total P were made both for Campoaves and Güres samples using QE65000 spectrophotometer (Ocean Optics) both at the laboratories of the University of Brescia (Italy) and University Politechnica of Bucharest (Romania), respectively. The measures were made using polystyrene cuvette (1 cm optical path) and evaluating the P wavelength (650 nm) in the visible domain (400 nm – 750 nm). The method followed the Romanian standardised method: STAS 9621-74 "COKE and SEMICOKE. Determination of phosphorus content", point 3, colourimetric method, variant II [33].

For all minor elements (0.1 %<wt. %<1 %), including Cu, Zn, Sr, Ba and some trace elements (wt.%<0.1%) including Mo, Pb, Ni, As, Cd, Sb, Au and Hg, the ash samples were digested with aqua regia (1:1:1 HNO_3:HCl:H_2O) followed by Inductively Coupled Plasma Mass Spectroscopy (ICP-MS) analysis at Bureau Veritas Commodities Canada Ltd. (Vancouver, Canada). To determine elements down to part per million level concentration in rocks, the analysis was made in the same laboratory after the ashes were fused with lithium tetraborate/metaborate followed by ICP-MS [34].

Detailed imaging experiments by Scanning Electron Microscopy combined with X-ray microanalysis (SEM-EDX) and optical microscopy

The SEM-EDX analysis was carried from raw samples, i.e. without previous preparation, and realised as petrographic analysis in polished blocks adapted according to ISO-7404-2 [35]. The experiments were done at Centro de Materiais da Universidade do Porto (CEMUP) using an FEI Quanta 400 FEG ESEM/EDAX Genesis X4M operated in low vacuum mode at 15 kV. The raw samples were adhered to the mounting block with double-sided adhesive carbon tape. The experiments were focused on the surface morphology via secondary electron detector mode (SE) alternating with backscattered electron detection mode (BSE) for different phases identification. For samples mounted on resin polished blocks, only the BSE mode was used to obtain detailed imaging of the particles internal structure. In both cases, EDX semiquantitative analyses were made in representative areas of the ash morphotypes. The optical microscopy analysis was carried out following sample preparation and measurements according to international standards (ISO-

7404-2), methodology and specific classifications of the International Committee of Coal and Organic Petrology. The experiments were done at University Politehnica of Bucharest (UPB-CPMTE) using an Olympus BX51M optical microscope, with the possibility of transmitting the image to a display with a CCD-1300QB model camera, in reflected and polarised light, glycerin immersion and 500 X magnifications.

Mineralogy by X-Ray Diffraction (XRD) analysis

The XRD analysis was carried at the University of Brescia (Italy). Powder of global samples was micronised and then analysed using an X'Pert PRO diffractometer (PANalytical, Malvern, UK) equipped with a Cu Kα anode (40 kV, 40 mA). The phases were determined using Philips X'Pert software (associated with the open crystallography database (COD)).

Results and Discussions

Sieving trials

After one sieving trial with the 5 mesh sieve and another with the 10 mesh sieve with Campoaves RHPL global sample, it was found that the 5 mesh sieve retains 23% of the material, while the 10 mesh sieve retains 46%.

The results of the granulometric distribution analysis carried by mechanical dry sieving for Güres ash samples are shown in Figure 2. The BA-GU sample is mainly (90 %) composed of the 1-2 mm and 2-4 mm size-fractions, which was confirmed during SEM experiments, while for FACYC-GU and FAECO-GU samples, the size distribution has a Gaussian shape. However, as the SEM experiment shows, sieving clog by small-size particles caused the overestimation of the 45-75 µm (e.g. Fig. 2D) and 25-45 size-fractions of FACYC and FAECO.

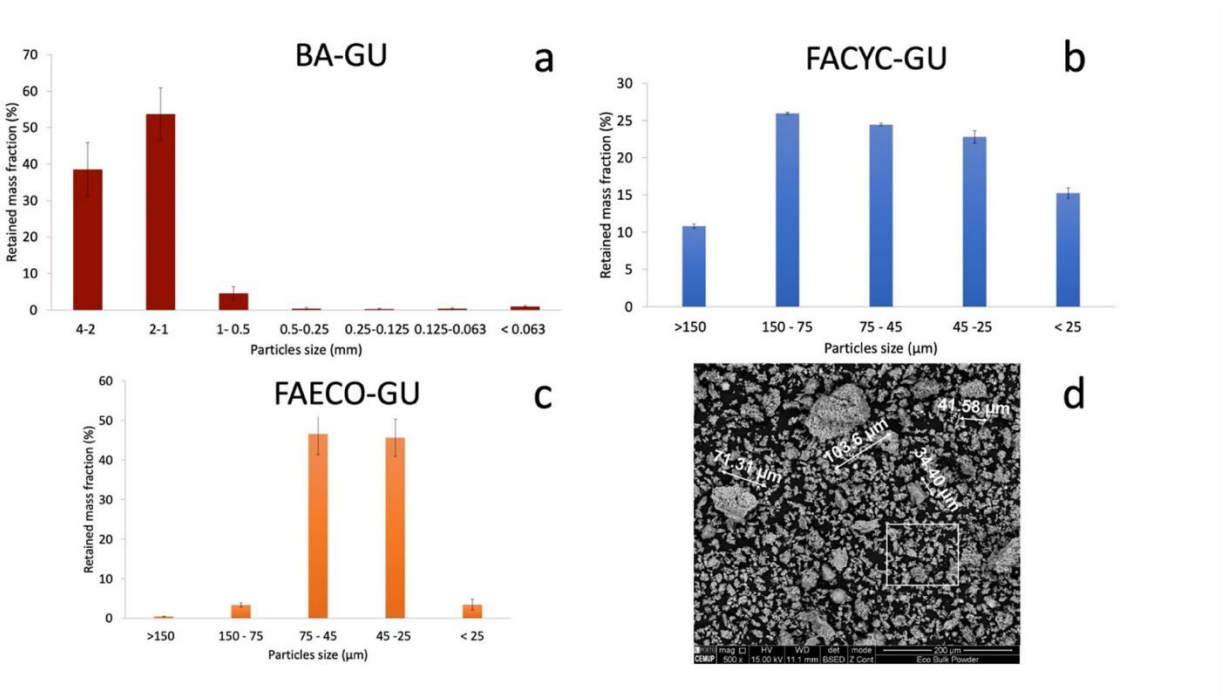

Figure 2. Size distribution analysis via mechanical dry sieving: A, B, and C) distribution of mass fraction (%) for Güres samples (number trials per each sample=5); D) SEM micrograph for FAECO-GU showing a background of micrometric and submicrometric particles there were also retained in the 325 mesh (45 µm) sieve due to sieve blinding (200×; BSE mode).

Proximate Analysis

The proximate analysis results of the fuel and the ash (BA, FAECO, FACYC) are presented in Table 1. Size-fractions are evaluated for the fuel in the case of Campoaves samples, meanwhile, for the ash they are evaluated in the case of Güres samples. These data are also plotted on a ternary diagram characterised by the comparison of three parameters for the proximate analysis (ash content, volatile matter, fixed carbon; Fig. 3) originally for biomass-based materials [23].

Sample		Moisture	Ash	Volatile Matter	Fixed Carbon
		(%)	(d.b. wt. %)		
Güres					
Fuel	Global	27.63	26.14	43.19	3.04
BA	Global	0.11	80.63	9.59	9.78
	4-2 mm	0.14	79.77	9.29	10.94
	2-1 mm	0.16	81.76	10.12	8.12
	1–0.5 mm	0.20	77.87	12.04	10.09
	< 0.5 mm	0.14	76.46	14.08	9.46
FACYC	Global	0.05	90.69	7.26	2.05
	> 150 µm	0.34	88.87	10.02	1.11
	150-75 µm	0.14	91.37	7.44	1.19
	75-45 µm	0.02	90.96	7.89	1.15
	45-25 µm	0.03	89.84	6.23	3.92
	< 25 µm	0.02	89.85	6.25	3.90
FAECO	Global	0.15	91.18	6.72	2.10
	> 75 µm	0.32	89.93	8.06	2.01
	75-45 µm	0.18	91.07	6.28	2.65
	45-25 µm	0.23	90.92	6.00	3.08
	< 25 µm	0.27	90.59	6.57	2.83
Campoaves					
Fuel	Global	37.42	11.20	49.64	11.93
	> 4 mm	30.84	9.65	51.67	11.45
	< 4 mm	26.86	9.24	51.27	12.25
	> 2 mm	27.74	10.57	50.28	11.92
	< 2 mm	47.78	17.29	35.74	19.74
BA	Global	9.50	45.14	19.35	8.29
FAECO	Global	3.54	57.25	11.61	3.92
FACYC	Global	3.18	61.91	9.71	1.57

All the values referred to Ash, Volatile Matter and Fixed Carbon are normalized with respect to one another reflecting data shown in the ternary plots in Fig. 3. (d.b. = dry basis)

Table 1 Results of proximate analysis and fixed carbon calculation from Güres and Campoaves ash samples.

Considering the fuel (RHPL and LHM) results, only the volatile matter values are similar for Campoaves and Güres global samples. Campoaves fuel contains higher moisture amounts and fixed carbon value (approximately four times), while Güres fuel contains two and a half more ash.

These results explain why the fluidised bed combustion may be the technology chosen to burn LHM, while RHPL can be burned in a chain grate stoker.

Significant differences characterise moisture, ash, volatile matter and fixed carbon among the size fractions of Campoaves RHPL. For a trial using the 5 mesh sieve, the fraction >4 mm, corresponds to 23 % of RHPL and contains approximately 25 % more moisture than the fine fraction. However, for a trial using the 10 mesh sieve, the fraction passing this sieve (<2 mm) corresponds to 54 % of the RHPL, and the coarser fraction (>2 mm) contains approximately double of the moisture, two times more ash and fixed carbon, and 1.5 times less volatile matter.

Such results are interesting to save energy with fuel drying, improve the incineration efficiency and obtain two or more ash categories, as sieving sand-size particles is an efficient and inexpensive separation method.

The amount of moisture in Güres global ash samples and respective size-fractions is residual (<0.34 %), while it is almost 10% in the case of Campoaves BA. Regarding the ash content, Güres FAECO and FACYC samples and respective size fractions contain approximately 90 % ash. In comparison, the ash percentage in Güres BA and respective size-fractions range between 76 % and 82 %, compensated by a higher rate of volatile matter and fixed carbon, most probably related to $CaCO_3$ sand relics decomposition during the analytical methods progress [36].

About Güres ashes, Campoaves ash global samples have much higher moisture percentages (about 10 % in the BA-CA sample), lower ash content (between 45 and 62 %), and a volatile matter content ranging between 10 and 19 %. However, the fixed carbon is similar to that of Güres global samples. All these differences are related to the manure composition and technologies: rice husk and wood chips contributing to higher volatile matter values in Campoaves ashes, the use of $CaCO_3$ sand bed contributing to higher ash content at Güres. However, the high amount of moisture and volatile matter found in the BA-CA sample are indicators of low-burning efficiency.

Vassilev et al. [24] reported that a classification based on a ternary diagram allows comparing biomass and biomass ash based on their proximate analysis (ash, volatile matter and fixed carbon). The RHPL and the LHM samples are plotted well inside the limits found by Vassilev et al. [24] for biomass (on a dry basis - d.b.: ash <40 %, volatile matter >40 %, and fixed carbon <20 %). However, Campoaves <2 mm, owing to its high volatile matter content and fixed carbon value (Fig. 3A), results out of the limit area.

In the case of the ash samples of the present study (Fig. 3), the dominant parameter here is the ash content which ranges between 45 % and 91 % with low volatile matter (<20 %) and fixed carbon (<11 %).

The BA-CA sample is the only ash sample plotted away from the other samples owing to its lower ash content and higher volatile matter (Fig. 3 A). Zooming out the ternary diagram (Fig. 3 B), three plotting areas can be noticed: the area of BA-GU sample and its size-fraction samples plotted around 10 % FC and 70-80 % ash; the Güres fly ashes (FACYC-GU and FAECO-GU global and size-fraction samples) with >89 % ash; and Campoaves fly ash samples (FAECO-CA, FACYC-CA), and outside the zooming also BA-CA, with low fixed carbon values (<13 %) but broader volatile matter and ash contents. Overall, the diagrams (Fig. 3 A and B) characterise very well the difference between the fuel and respective ashes, the bottom ash and fly ash, and ashes from different fuels and technologies.

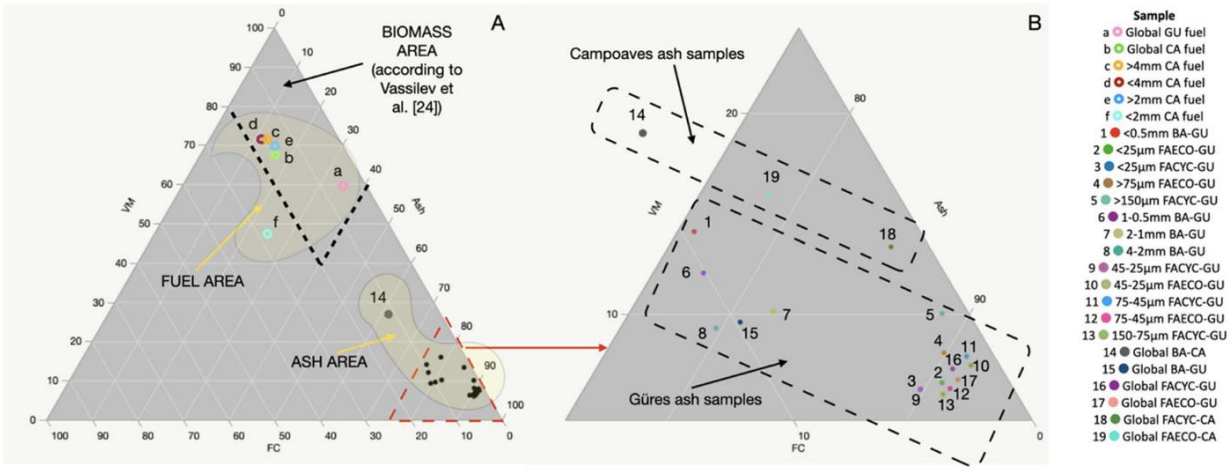

Figure 3. A) Positions of ash samples in a classification system based on data from proximate analysis; Dashed black lines are the limits of biomass in Vassilev et al. [24]. B) zoom of dashed red area in "A". Abbreviations: VM, volatile matter; FC, fixed carbon. The parameters are all expressed with d.b. wt.%. A ternary diagram was made with JMP software.

Elemental Analysis

The results of the major oxides determination for Güres and Campoaves ash samples are presented in Table 2. These are similar to other concentrations reported for ash derived from the incineration of animal by-products [26, 28, 37, 38]. However, the P_2O_5 concentrations of the ash samples studied are within the range of mined phosphate rock grades, especially the medium-low

346 grade phosphate rocks [39, 40)]. For instance, they are lower than grades from the best
347 sedimentary ores from Morrocco or Jordan, reaching 30 to 38 %. Grades in these latter deposits
348 increased during the last decade thanks to technological improvements (Steiner et al., 2015).
349 The major oxides analysis highlights fundamental differences between Campoaves and Güres, but
350 also between the BAs and respective FAs:
351 (1) the concentration of SiO_2 is much higher in Campoaves ashes due to the SiO_2 layer in the
352 rice husk used as poultry bedding, while the hens are kept inside cages at Güres;
353 (2) the concentration of CaO is approximately five times higher in Güres ashes since $CaCO_3$
354 sand is used to capture S in the fluidised bed chamber, and also due to eggshells;
355 (3) the K and P oxides follow the concentration trends: BA<FAECO<FACYC at Campoaves, and
356 BA <FACYC<FAECO at Güres. This evolution is related to the position of each sampling location
357 (Fig. 1) since coarse particles tend to be collected firstly by the dust capture equipment. As the
358 flue gas cools, condensation reactions occur on finer particle surfaces. Campoaves rice husk relics
359 are the dominant particles of the ashes. In contrast, at Güres, coarse particles are mainly $CaCO_3$
360 sand particles more or less decomposed with (Ca-P-K-S)-rims developed on them, and in both
361 cases, the fine particles are composed of neo-formed morphotypes (or rims fragments) K- and P-
362 rich.
363 For both Campoaves and Güres samples, the BA samples' LOI and total C values are very high and
364 approximately double that in the FAECO and FACYC samples. The relatively low amount of P_2O_5 in
365 the BA may be related to the combustion efficiency in the case of Campoaves. In contrast, in the
366 case of Güres, it is related to combustion technology, i.e., the utilisation of a fluidised bed
367 composed of $CaCO_3$.
368 Vassilev et al. [41] proposed a second classification for the materials derived from biomass to give
369 additional information on potential applications of the ash. For example, from the combustion
370 process perspective, it provides indications on how to deal with technological problems such as
371 corrosion, accumulation of materials inside the ducts (cloggings, foulings). This scheme was
372 developed for the present samples due to their biomass-based nature and incineration, which
373 yield similar features to ashes obtained after coal burning.
374 Figure 4 shows the Vassilev 's classification under three categories (C, S, K types). Campoaves
375 samples are close to the "K-type" typical of materials containing phosphates, sulphates, chlorides
376 and amorphous material. They have alkaline pH and water-soluble components (Cl, K, Na, Ca) that
377 indicate they could be suitable soil improvers in acidic soils. On the other hand, the constituents

have low-T melting that can affect biomass processing. Güres samples, instead, are located in an area shared between C-type and CK-type, characteristic of Ca-bearing minerals. They have an alkaline pH with possible low melting T compounds during combustion, so they should be taken into account for the constant deposition of material on the internal surface of ducts [42].

Both Güres and Campoaves samples are far from the S type area, typical of more acidic materials which consist of detrital minerals (e.g., silicates) characterised by higher stability during weathering and chemical elements less mobile in water.

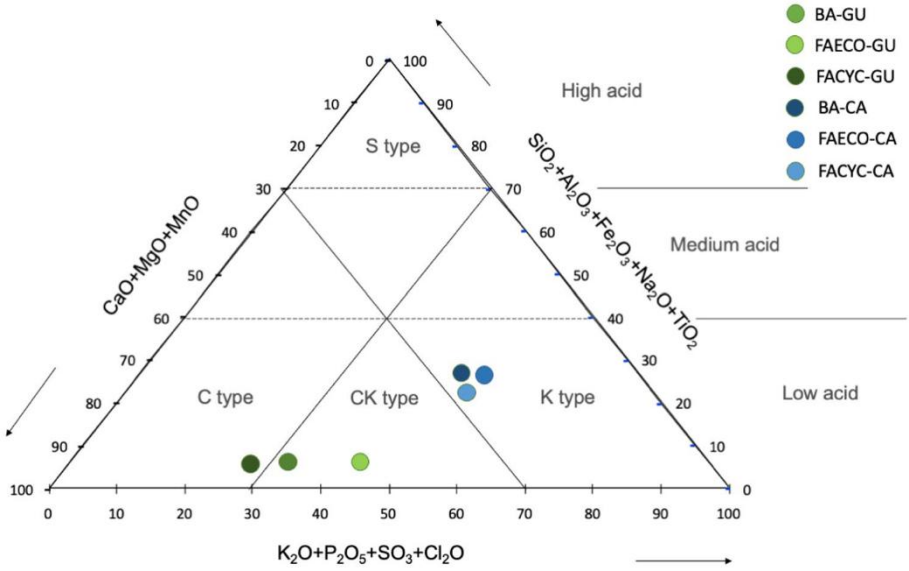

Figure 4. Ash analysis under the classification method reported by Vassilev et al. for biomass materials [41]. All the parameters are expressed in wt.%. Ternary diagram was made via XLSTAT plug-in for Microsoft Excel.

	Campoaves*			Güres		
	BA	FAECO	FACYC	BA	FACYC	FAECO
SiO_2	11.2	14.5	12.7	2.1	2.4	1.6
Al_2O_3	0.7	0.8	1	0.3	0.3	0.3
Fe_2O_3	0.7	0.7	0.9	0.4	0.5	0.7
CaO	9.9	10.3	12.3	48.3	47.7	36.2
MgO	5.4	5.8	8.2	3.1	5.6	6.3
Na_2O	2.5	2.9	3.3	1.3	2.1	2.5
K_2O	14.4	>15	>15	6.5	6.8	12.2
MnO	0.3	0.3	0.4	0.1	0.2	0.2
TiO_2	0.04	0.05	0.06	0.03	0.04	0.03
P_2O_5	12.8	13.3	17.6	9.3	17.5	17
SO_3	2	8.7	6.9	4.7	4	8
Cr_2O_3	<0.01	<0.01	<0.01	<0.01	<0.01	<0.01
Ba	<0.01	0.03	0.03	<0.01	<0.01	<0.01
Sr	<0.002	0.009	0.017	0.051	0.047	0.053
LOI	40.7	22.1	17.2	22.8	12.1	14
C_t	21.6	15.1	10	5	2.2	1.9
S_t	1	3.1	2.6	1.9	1.6	2.8

Major elements determined with X-ray fluorescence analysis on fused lithium tetraborate/metaborate discs

*Campoaves 2nd sampling (14Jun2019); LOI—loss on ignition; Ct—total carbon; St—total sulphur. All the value are expressed in wt%

Table 2. Elemental composition of laying hens manure ash from Güres (BA, FAECO, FACYC) and rice husk poultry litter ash from Campoaves (BA, FAECO, FACYC). Major elements determined with X-ray fluorescence analysis on fused lithium tetraborate/metaborate discs.

Total Phosphorus determination, minor and trace elements

Table 3 lists the results of Total P and trace elements determination. The P-trend is the same found for P_2O_5, i.e., P is more concentrated in the fly ashes, but the increase downward the flue gas stream is not evident in the case of Güres fly ashes. However, the values are comparable with the P content in medium-low grade phosphate rocks [33,34].

Most of the elements determined by ICP-MS are present at low concentrations. For example, the sum of total Rare Earth Elements plus yttrium (REE+Y) ranges between 21 ppm for the FAECO-GU sample and 7 ppm for FACYC-CA. The higher REE+Y and Th and U concentration on the Campoaves

samples may be related to the rice husk used for the bedding [43–46] since the fertilisers used on rice fields are enriched in REE, U and Th from the phosphate rocks.

Some elements such as Cu, Zn, Ba, Rb, Sr are present in higher concentrations with contents up to 2516 ppm in the case of Zn. Meanwhile, many elements (the exceptions are W and REE+Y) are present in higher concentrations in the fly ashes. Some chemical elements have their concentration increasing in the stream downwards due to their volatilisation and condensation when the gas cools (e.g., Se) and their occurrence as fine particles.

		Campoaves			Güres		
		BA	FAECO	FACYC	BA	FACYC	FAECO
*Colorimetry (wt.%)	*TP	4.4	5.2	7.8	3.8	8	7.9
Lithium tetraborate/ metaborate fusion, ICP-MS (ppm)	Ba	133	155	190	39	77	80
	Be	<1	<1	<1	<1	<1	<1
	Co	2.6	3.2	4.4	4.3	5.1	7.9
	Cs	0.3	1.0	0.9	<0.1	<0.1	0.8
	Ga	0.9	1.1	1.1	<0.5	<0.5	<0.5
	Hf	0.3	0.5	0.4	0.1	0.3	0.2
	Nb	1.1	0.6	1.0	0.2	0.3	0.3
	Rb	69	149	129	40	34	93
	Sn	<1	2	2	<1	<1	<1
	Sr	123	138	200	753	652	773
	Ta	<0.1	<0.1	<0.1	<0.1	<0.1	<0.1
	Th	0.8	1.0	1.1	0.3	0.2	0.4
	U	29	32	35	0.6	0.7	1.1
	V	36	30	42	<8	<8	<8
	W	4.7	2.2	3.7	<0.5	<0.5	6
	Zr	15	19	18	5	12	5
	La	2.6	2.8	3.4	1.5	1.8	1.4
	Ce	3.8	4.5	5.0	1.8	2.0	1.9
	Pr	0.4	0.5	0.6	0.2	0.2	0.2
	Nd	1.8	2.1	2.2	0.9	0.9	1.0
	Sm	0.3	0.4	0.4	0.1	0.2	0.2
	Eu	0.1	0.1	0.1	0	0	0
	Gd	0.3	0.4	0.5	0.2	0.2	0.2
	Tb	0.1	0.1	0.1	0	0	0
	Dy	0.4	0.4	0.5	0.2	0.2	0.2
	Y	5.3	5.8	6.8	1.4	1.2	1.2
	Ho	0.1	0.1	0.1	0	0	0
	Er	0.4	0.4	0.5	0.1	0.1	0.1
	Tm	0.1	0.1	0.1	<0.01	0	0
	Yb	0.7	0.8	0.9	0.1	0.1	0.1
	Lu	0.2	0.2	0.2	0	0	0
	ΣREE + Y	16.5	18.5	21.4	6.6	7	6.5
Aqua Regia digestion (1:1:1 HNO_3:HCl:H_2O), ICP-MS (ppm)	Mo	18	19	25	6	9	13
	Cu	393	430	488	137	208	297
	Pb	0.7	3.9	3.9	0.4	1.4	4.2
	Zn	838	2516	2221	994	1120	2356
	Ni	32	37	54	19	20	42
	As	0.6	1.7	<0.5	3.1	1.4	6.1
	Cd	0.1	2.8	1.8	<0.1	0.7	2.0
	Sb	0.1	0.3	0.4	0.4	0.3	0.7
	Bi	<0.1	<0.1	<0.1	<0.1	<0.1	<0.1
	Ag	<0.1	<0.1	<0.1	<0.1	<0.1	<0.1
	Au (ppb)	<0.5	<0.5	0.6	1.8	0.5	1.2
	Hg	<0.01	<0.01	<0.01	<0.01	<0.01	<0.01
	Tl	<0.1	<0.1	<0.1	<0.1	<0.1	0.3
	Se	1.8	3.5	12.7	0.6	1.9	6.5

*TP stands for total phosphorus and the colorimetric method was done by UV–VIS spectrophotometer

Table 3. Total phosphorus determination and minor and trace composition of laying hens manure ash from Güres (BA, FAECO, FACYC) and rice husk poultry litter ash from Campoaves (BA, FAECO, FACYC).

Ash Mineralogy and Morphology

The results of the XRD analysis of the ash samples that include the determination of the amorphous and crystalline phases are shown in Fig. 5. In Güres samples, the main crystalline phases are those containing Ca, such as hydroxyapatite ($Ca_5(PO_4)_3(OH)$), calcite ($CaCO_3$), calcium hydroxide (CaOH) and lime (CaO). These Ca-crystalline phases, specifically of $CaCO_3$ sand, and minor amounts of associated dolomite ($MgCO_3$), result in the fluidising bed during combustion for the neutralisation of S. The Ca content is high because Ca it is an essential diet for the laying hens and concentrates in the excrements. Consequently, phosphorus combined entirely with Ca and formed hydroxyapatite. Meanwhile, other minor phases were also determined at Güres: a complex form of Si-containing Na, Mg and K is also present, which is probably related to a small fraction of quartz sand used during the early stages of the boiler heating that combine with volatilised Na, Mg and K; Mg is oxidised mostly as periclase in the combustion chamber and is carried by the flue gas; portlandite ($Ca(OH)_2$), formed due to the decomposition of calcite ($CaCO_3$) into calcium oxide (CaO) and the subsequent interaction of CaO with the moisture (H_2O); finally, when comparing the different ashes from Güres one may see that sylvite (KCl) amount is higher in the fly ash, this is a consequence of Cl, and K reaction as the flue gas cools leading to sylvite condensation on the surface of the fly ash particles.

The mineralogical composition of Campoaves ashes is also quite different from Güres BA owing to the reduced amount of Ca leading phosphates to form different compounds. Campoaves ashes are mainly composed of amorphous materials, and the crystalline phases are primarily composed of arcanite (K_2SO_4), hydroxyapatite and other forms of P-bearing minerals and sylvite (KCl). However, these phases are not equally distributed among all Campoaves ashes. In the bottom ash, other forms of P-bearing minerals (tricalcium phosphate ($Ca_3(PO_4)_2$) and K-struvite ($KMgPO_4(6H_2O)$)) equal hydroxyapatite, indicating a low-combustion efficiency since some of these phosphates may have formed at atmospheric temperature.

The Na-phosphate (NaH_2PO_4) and sodium hydrogen phosphate hydrate [$Na_3HP_2O_7(H_2O)$], also found in Fiameni et al. [37], is a residual phase in BA but is significant in FAECO and FACYC samples. Low-temperature (α-)quartz (probably a polymorph) and amorphous SiO_2 are expected phases at Campoaves ashes since the aviary bedding is composed of rice husk that contains Si.

454 Meanwhile, K-sulfate is more dominant than sylvite at Campoaves due to a higher K to Cl ratio for
455 a given amount of sulfate and because S is not captured inside the combustion chamber like in
456 Güres. Finally, Mg-based phases (e.g., periclase) are absent in Campoaves, indicating that most Mg
457 reacts with phosphates in the combustion chamber.
458

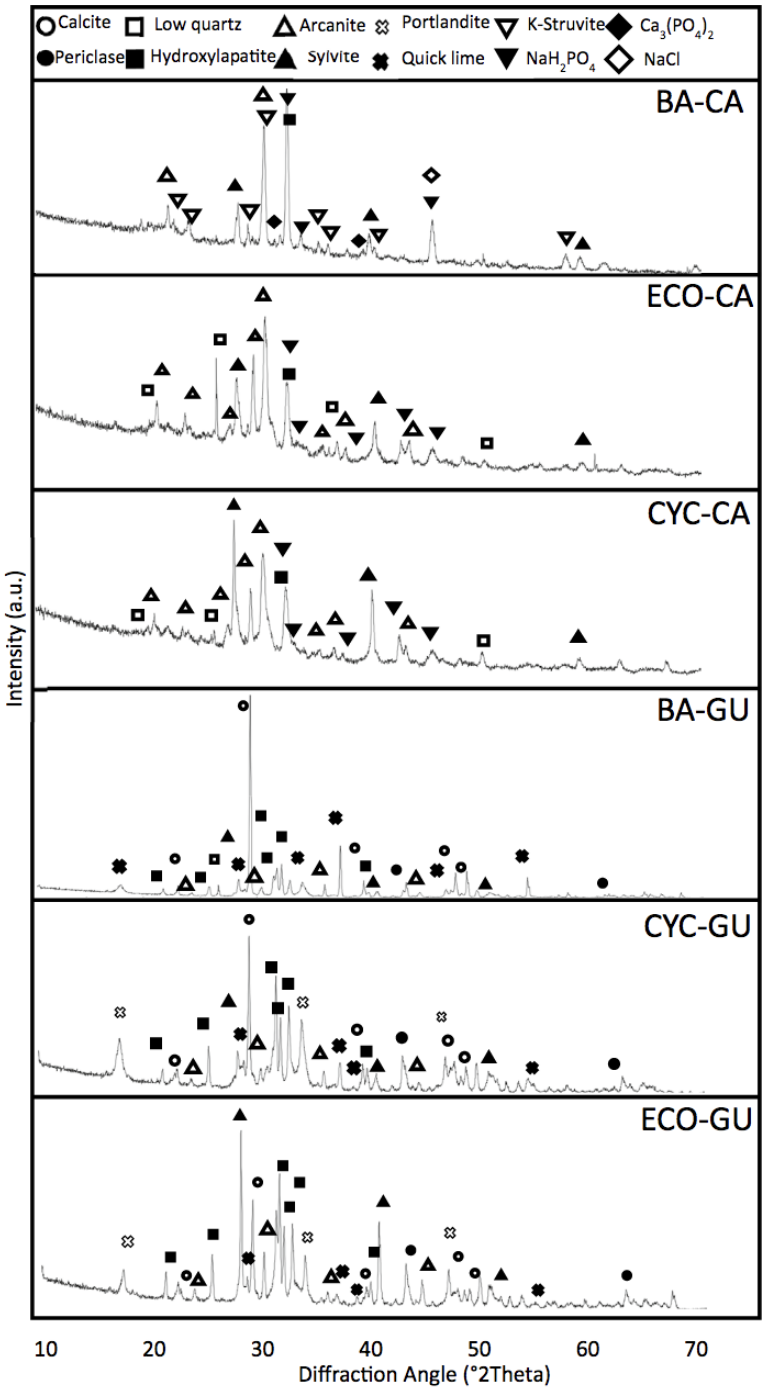

459
460
461
462 Figure 5. XRD spectra with the mineralogical identifications of Güres and Campoaves samples

Detailed imaging experiments by Scanning Electron Microscopy combined with X-ray microanalysis (SEM-EDS)

Detailed imaging and X-ray microanalysis via SEM-EDS experiments allowed us to corroborate the particle size distribution, chemical analyses and the phases determined by XRD.
SEM-EDS images for Campoaves are reported in figures 6-7-8-9, while for Gures are reported in figures 10-11-12-13-14-15.

The RH is composed of a low-temperature Si-layer intimately attached to thick-wall cells, and the poultry excreta attaches to the outer surface of the husk or fills in the void left by the rice grain (Fig. 6 A-C). This way, Campoaves BA is mainly composed of partially baked RH (Si and unburned C) mixed with partially baked poultry excreta (Fig. 6 D-F), which are the components of the amorphous P and SiO_2 phases and unburned carbon.
The melting of the RH silica with P and other elements from the poultry excreta generates millimetric P-rich morphotypes composed of neo-formed crystalline and amorphous phases of P-Ca blebs embedded in a silicate matrix with K, Mg and Ca (and residual Fe and Al) (Fig. 6 G-L). Therefore, chemical compounds such as $KMgPO_4(6H_2O)$ and CaO, MgO, sulfates, and chlorides can be found at the particle surfaces.

The size analysis of on Campoaves FAECO sample shows that this material is mainly composed by three size fractions (Fig. 7 A, C and G): >500 µm; between 75 and 250 µm; and <75 µm, mainly composed of fragments of particles identified in the other size-fractions.
The >500 µm size-fraction consists of two main morphotypes: partially baked RH relics with approx. 1.5 mm length, Si-crenulated outline, semi-detached unburned carbon and a thin Si-internal layer (Fig. 7 B); large (approx. 500 µm) P-rich rounded morphotypes (phosphospheres) composed of P-Ca blebs embedded by a (K, Mg, Ca)-silicate matrix (Fig. 7 G and H).
The 75-250 µm size fraction (Fig. 7 C and G) is composed of baked fragments of the RH Si-materials, Ca-idioblasts relics from the wood chips (Fig. 7 C and D), partially baked poultry excreta without Si (Fig. 7 C and E), and (Si-Ca-K-Mg)-phosphospheres, some with quartz inclusions (Fig. 7 C and F).

Although Si is not found in some partially baked particles of poultry excreta (Fig. 7 G and I), all analysed P-rich spherical morphotypes contain Si (Fig. 7 G, H, J-L). Some Si from the RH silica must react with the poultry excreta while Ca binds with Si and P forming Ca-P blebs cement by a Ca-silicate. Like K, some P de-volatilise and react with S forming P-sulphate, which on cooling condensates at the surface of the particles. However, the main compounds of these condensation reactions are 1-2 µm rims composed of K-sulphate and KCl (Fig. 7 J-L). Therefore, it might be possible that most devolatilized P is released into the atmosphere.

At Güres, however, the $CaCO_3$ sand decomposition releases calcium and CO2, recombining to capture S, P and K and forming thick rims around the sand grains. The presence of calcite explains why the end-products are different from those from Campoaves.

The fraction <75 µm from the Campoaves FACYC sample is characterised by fragments of partially to entirely baked poultry excreta, Si- P- and Ca-rich spheres and fragments of biochar, Si from RH, and Ca-oxide grains (Fig. 8 A). The particle above 75 µm RH biochar and Si-relics, phosphospheres (Fig. 8 A and B), Ca-idioblast relics from wood chips (Fig. 8 E), partially baked poultry excreta (Fig. 8 F and G), and bone fragments (Fig. 8 H and I).

Campoaves phosphospheres

Phosphospheres are one of the main P-source in Campoaves fly ash, but there is no evidence of phosphospheres in BA, only RH relics and partially baked excreta (Fig. 9 A). The SEM-EDS experiments carried on FAECO show abundant phosphospheres with diameters ranging from approx. 100 to 500 µm, composed of P-K-Ca blebs embedded by an Mg-Si-Al matrix (Fig. 9), is related to the high amount of Si available from the rice husk and is a distinctive characteristic of these ashes.

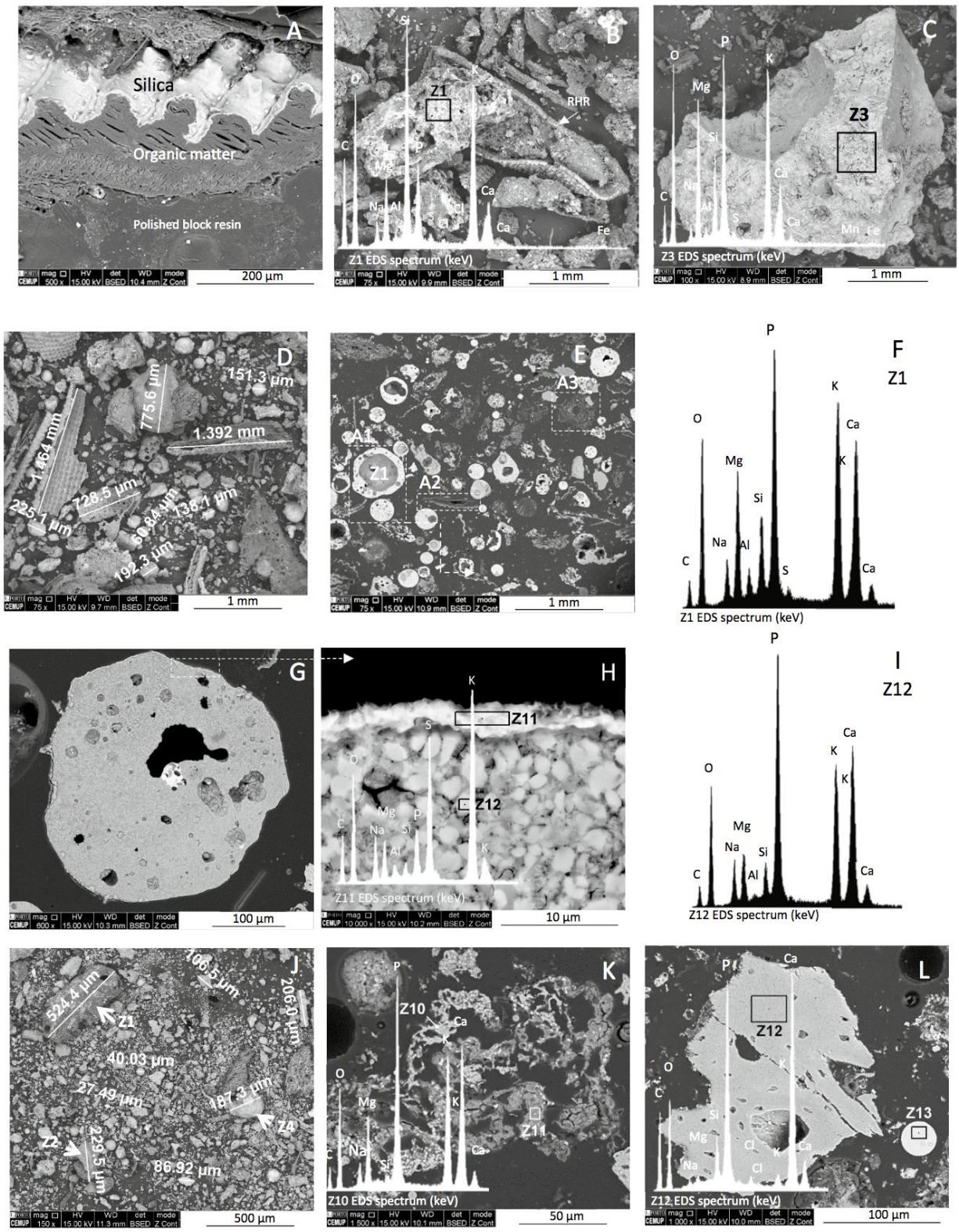

Figure 6 Micrographs and EDS spectra of rice husk (RH) in the fuel of "Campoaves" (Figueira da Foz, Portugal) and respective bottom ash (BA) (SEM-EDS BSE mode): A) cross-section of one RH measuring approx. 3×3 mm (×65; polished block); B) magnification of dashed square in "A" detailed image of the organic matter and silica layers in RH (×500); C) EDS spectrum in the dashed square in "B", with major Si and O peaks and residual K; D) Bottom ash, a silicate-rich particle with sulfates

529 and KCl at the surface (Z1 EDS spectrum), and below this a partially baked RH relic (RHR; ×75;
530 global sample); E) Bottom ash, partially baked poultry excreta (×95; polished block); F)
531 magnification of dashed square in "E" detailed image of partially baked P-rich fraction in poultry
532 litter excreta (×500); G) Bottom ash, irregular-shaped (P-K-Mg)-rich morphotype (×100; global
533 sample); H) cross-section showing the internal structure of an irregular-shaped P-rich morphotype
534 (×2500; polished block); I-L) EDS spectra in "H" to show the chemical composition of the silicate
535 matrix (Z2 and 3), the embedded P-blebs (Z4), and a residual Fe sulfate grain (Z5).

536

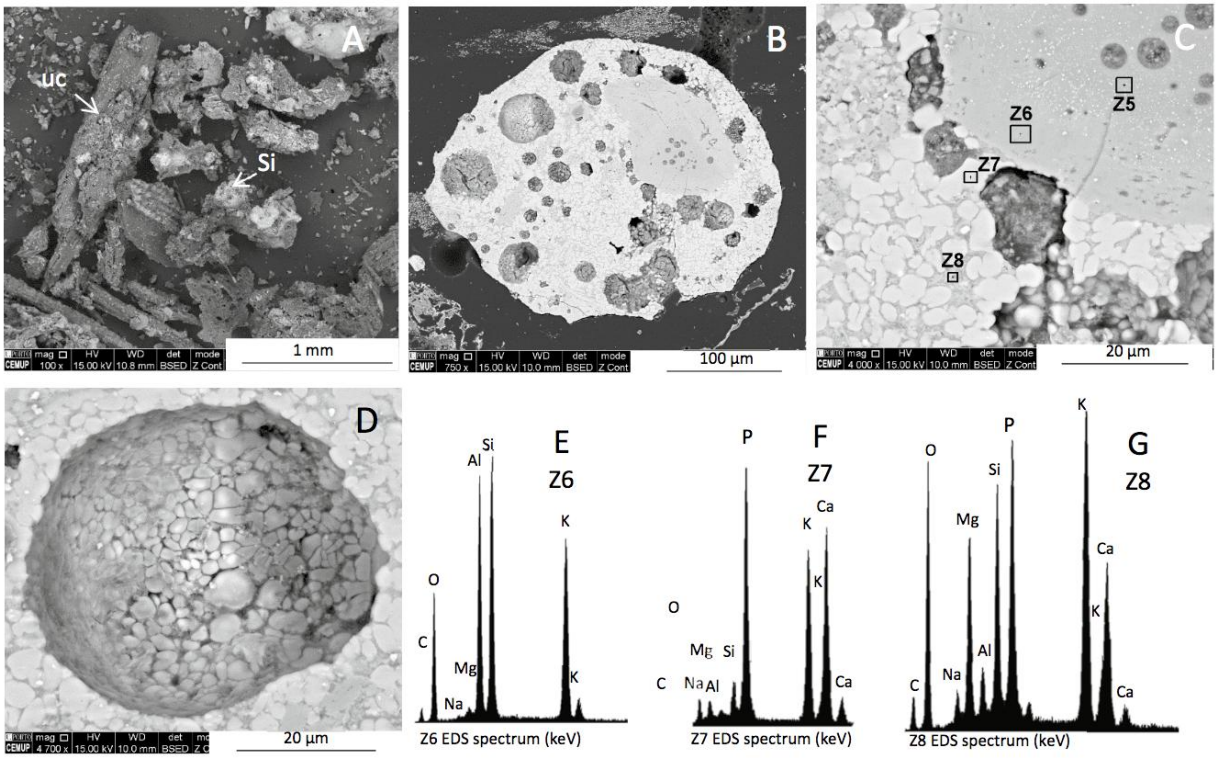

537

538

539 Figure 7 Micrographs and EDS spectra of "Campoaves" (Figueira da Foz, Portugal) Economizer fly
540 ash (FAECO) (SEM-EDS BSE mode): A) overview and particles measurement (×75); B) unburned
541 carbon and silica layers in RH relic (×200); C) overview of the 75-250 µm with marked EDS areas; D)
542 Z7 EDS spectrum in "C" of a Ca-idioblast relic from wood chips; E) Z8 EDS spectrum in "C" of an
543 irregular Si-poor P-(Ca-Mg-K)-rich morphotype; F) Z9 EDS spectrum in "C" of a rounded Si-rich P-
544 (Ca-Mg-K)-rich morphotype; G) polished block overview showing the main morphotypes: A1 dense
545 and hollow phosphospheres (EDS spectra Z1 marked), A2 RH relics, A3 partially baked poultry
546 excreta (×75); H) Z1 EDS spectrum in "G"; I) partially baked poultry excreta and EDS spectrum with
547 major Mg, P and K peaks, and without Si and Ca (×1000); J) cross-section of a phosphosphere and

Z11 EDS spectra in “K” (×600; polished block); K) magnification of “J”, the surface is composed of K-sulfate (Z1), while the interior is composed of P-K-Ca-blebs embedded by a silicate matrix (×10000); L) EDS spectra in “K” showing the chemical composition of P-blebs (Z12).

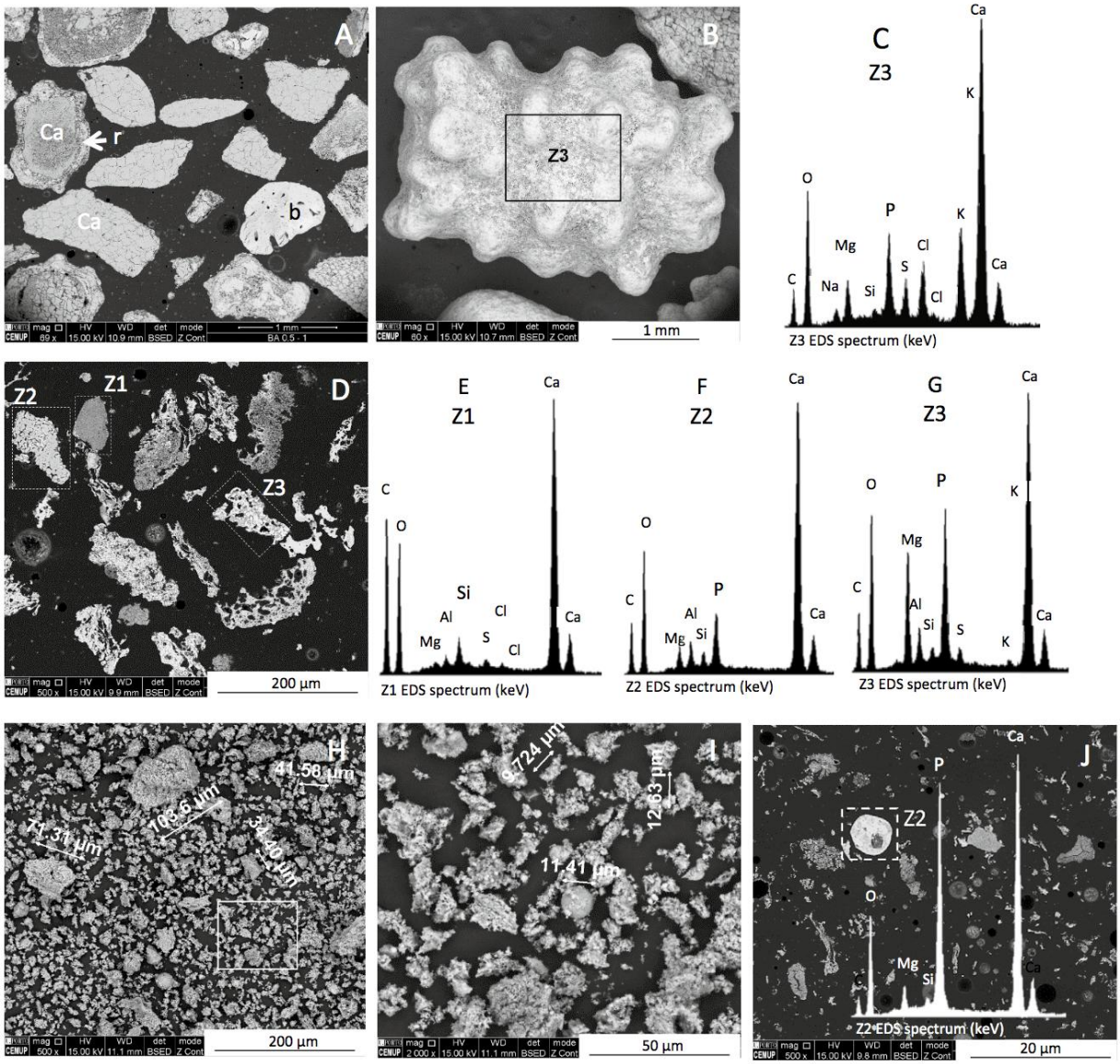

Figure 8 Micrographs and EDS spectra of “Campoaves” (Figueira da Foz, Portugal) Cyclone fly ash (FACYC) (SEM-EDS BSE mode): A) overview, particles measurement and EDS measured areas (×150); B) Z1 EDS spectrum in “A” of an unburned carbon particle; C) Z2 EDS spectrum in “A” of a Si-relic from RH; D) Z4 EDS spectrum in “A” of a phosphosphere; E) Ca-idioblast relic from wood chips and respective EDS spectra; F) partially baked poultry excreta. A mixture of P-K-Ca (Z10 EDS spectrum) and Si in darker portion (Z11) (×1000); G) Z11 EDS spectrum in “F”; H) bone fragment and small Si-rich K-Ca-P-Mg sphere (×1000); I and J) EDS spectra Z12 and Z13 in “H”.

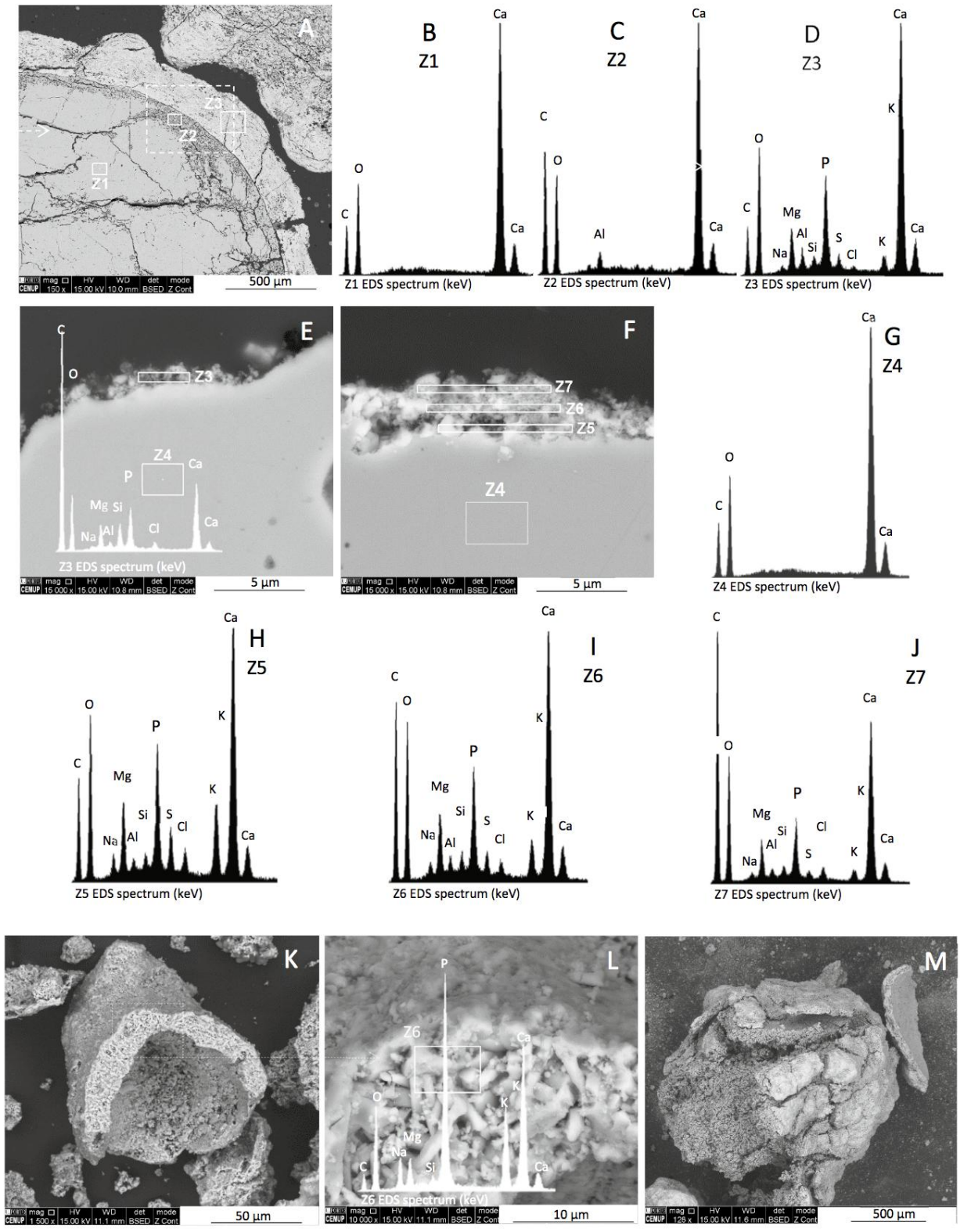

Figure 9 P-inorganic amorphous and phosphospheres in Campoaves bottom ash, Economizer (FAECO) and Cyclone (FACYC) fly ash samples (polished blocks; SEM-EDS BSE mode): A) overview of bottom ash: rice husk relics with silica (Si) and unburned carbon (uc) (global sample; ×100); B) overview of FACYC with rice husk relics (RH) and phosphospheres (pho) (×75); C overview of FAECO with rice husk relics (RH) and phosphospheres (pho) (×75); D) overview of FACYC (×75); E)

phosphosphere with pomegranate structure and silicate inclusion (×750); F) magnification of pomegranate structure in "E" with marked EDS spectra areas (×4000); G) magnification of hole in "E" with P-blebs (×4700); H) EDS spectra Z6 in "F"; I) EDS spectra Z7 in "F"; J) EDS spectra Z8 in "F".

The main characteristic of Güres BA is its content in particles similar to those of the $CaCO_3$ sand (Fig. 10 A). Many of these are covered by a thick layer composed of sulphates and chlorides (Fig. 10 B-D). Some sand may still be almost pristine, while other is already under decomposition (Fig. 10 E-F). However, some particles have a core made of bone or miscellaneous material (Fig. 10 E-F).

Güres FACYC sample granulometry ranges from <25 µm to >200 µm particles, corroborating the sieving analysis. The morphotypes composition is quite heterogeneous, including fragments of $CaCO_3$ sand (pristine or decomposed), rims of S, K and P retention, bone fragments, RH relics, partially baked excreta, and phosphospheres (Fig. 11).

The measurement of particles on the Güres FAECO sample confirms that this material is composed of three size fractions (Fig. 12 A-B), but the most abundant is the one below 25 µm. The coarse particles are mainly decomposed $CaCO_3$ sand fragments and some phosphospheres (Fig. 12 C-H). In contrast, the fine fraction is almost entirely composed of rough Ca-P particles and decomposed $CaCO_3$ sand fragments covered by sulfates and chlorides (Fig. 12 I-K).

Decomposition of $CaCO_3$ sand and P-rich rims formation

The $CaCO_3$ sand is used in fluidising bed combustion to capture S, forming calcium sulfate. One can see in Fig. 13 A-I that $CaCO_3$ sand decomposes and cracks from its surface to the interior while Ca moves to the surface and reacts with S, K, and P, among other elements, forming a rim. With time the particle becomes an "old" grain from cryptic $CaCO_3$, the edge detaches (Fig. 13 J and K).
The rim formed around the $CaCO_3$ sand may start with a micrometric layer of Na, S, Ca, and K sulfates (Fig. 14 A-C), which then alternate and include amorphous and crystalline Ca-phosphate (Fig. 14 D-H).

Güres phosphospheres

The main origin of P in Güres ashes is related to P-rich rims formed around $CaCO_3$ sand and amorphous particles probably formed from partially baked laying hens manure. Glassy P-rich spheres (phosphospheres) seem scarce (Fig. 15 A and B), and the ones observed have a composition similar to the one of partially baked laying hens manure, i.e. with dominant Mg, P and Ca and residual Si and Al (Fig. 15 C-K).

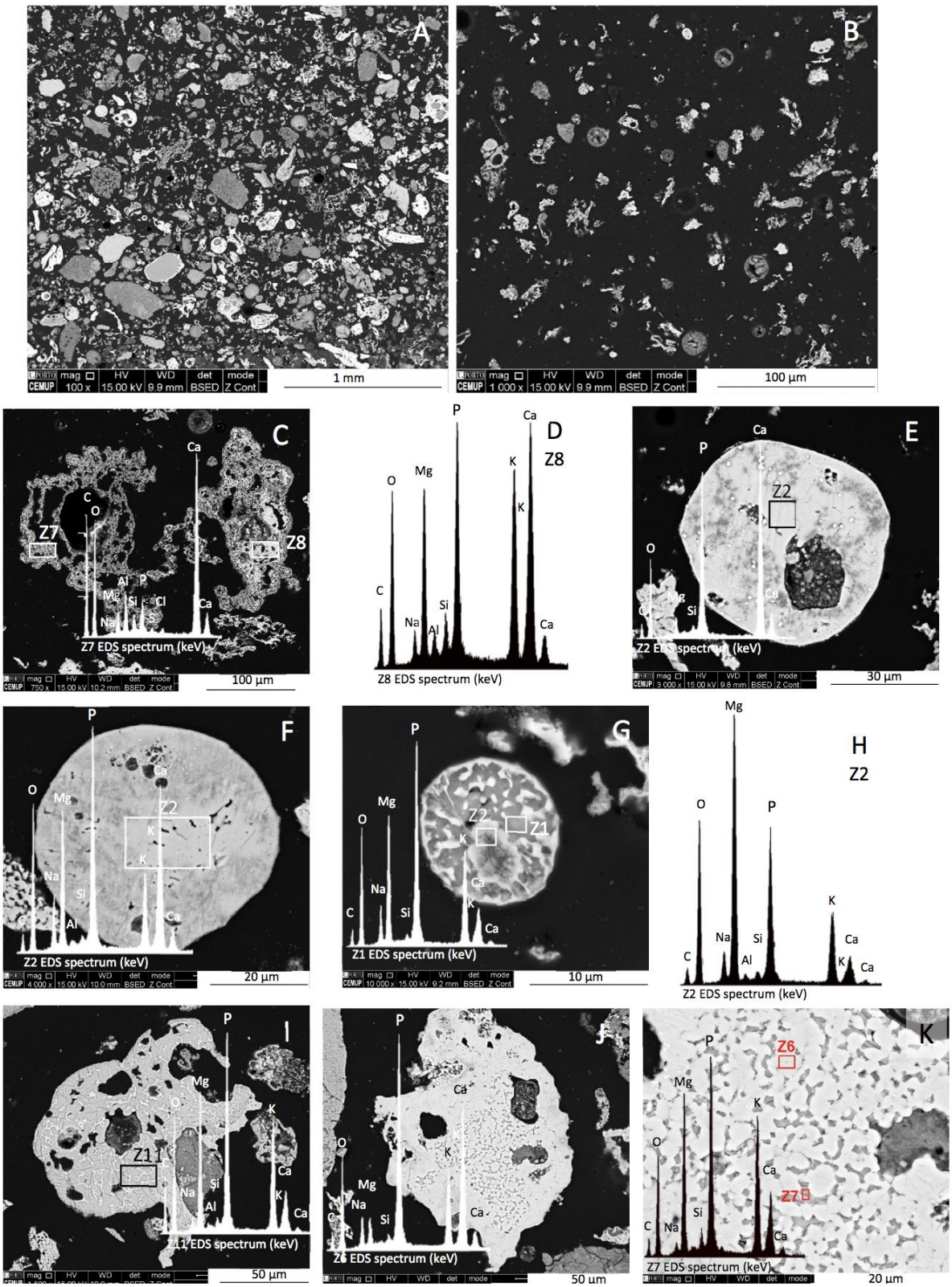

Figure 10 Micrographs and EDS spectra of “Güres” (Turkey) bottom ash (SEM-EDS BSE mode): A) polished block overview: $CaCO_3$ sand (Ca) with and without rim (r), and bone fragment (b) (×69); B) particle covered by a rim (global sample; ×60); C) Z3 EDS spectrum in “B”; D) fragmented $CaCO_3$ particle showing a thick rim (global sample; ×44); E) $CaCO_3$ particle without rim (polished block;

×100); F) old $CaCO_3$ particle fragmented and showing with heavy signs of reaction (polished block; ×128); G) bone fragment with rim (polished block; ×100); H) particle with miscellaneous nucleus and rim (polished block; ×100).

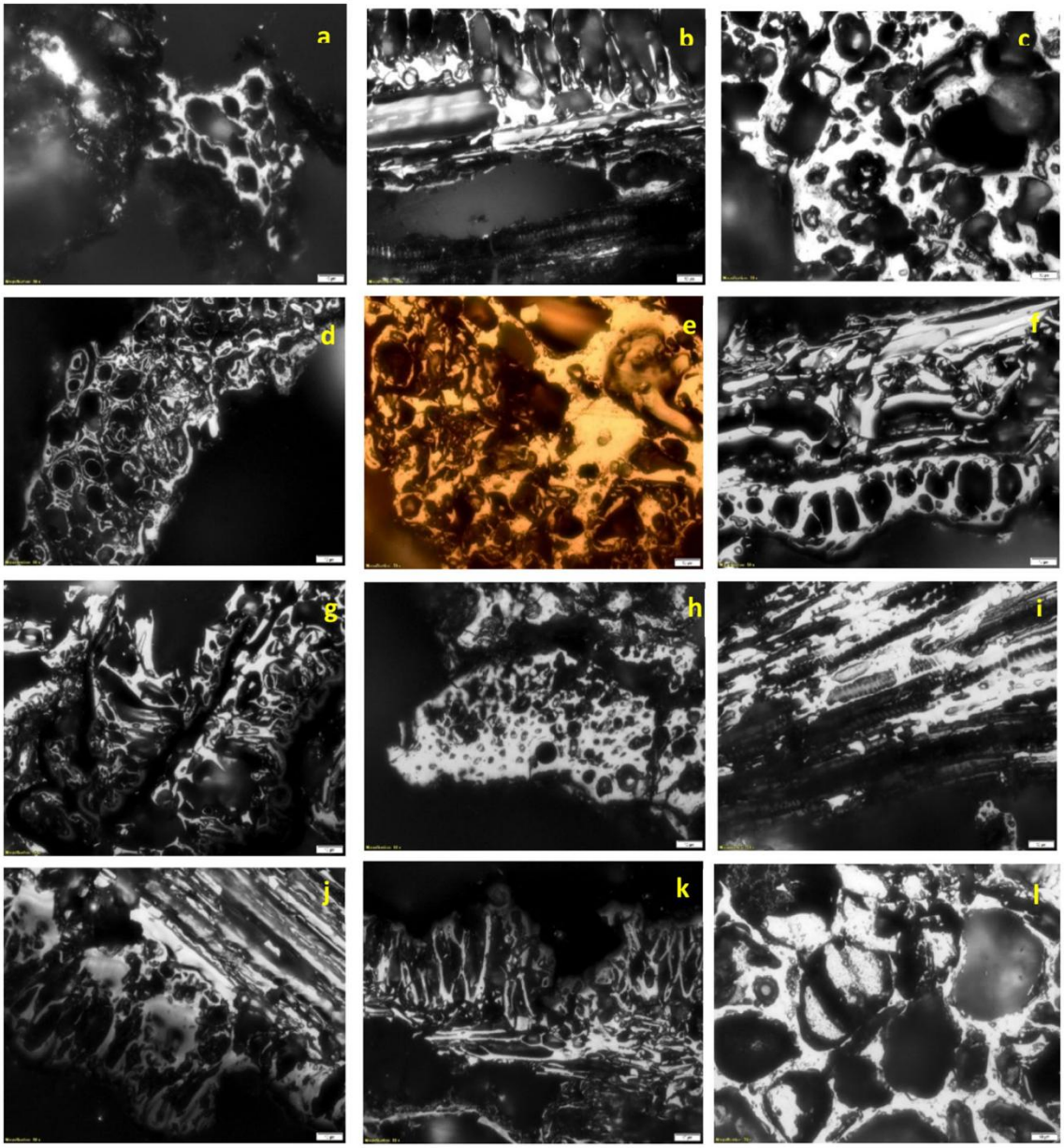

Figure 11 Micrographs and EDS spectra of "Gures" (Turkey) Cyclone fly ash (SEM-EDS BSE mode): A) polished block sample overview with marked common coarse morphotypes: $CaCO_3$ sand (Ca), P-rich subrounded particle (pho), and bone fragment (b) (×500); B) polished block sample overview with marked common middle-size morphotypes: $CaCO_3$ sand (Z1), Ca-fragment with P (Z2), and irregularly-shaped and networked particle of Ca-P-Mg (Z3) (×500); C-E) EDS spectra Z1, Z2 and Z3 in "B"; F) global sample overview of coarse particles (>150 µm) includes rice husk relics (RH), bone

622 fragments (b) and P-rich particles (pho) covered by KCl and MgO (×100); G) rice husk relic (polished
623 block; ×650); H) irregularly shaped with networked structure particle composed of Ca-Si-P and
624 minor concentrations of Na, Mg and K (polished block; ×500).

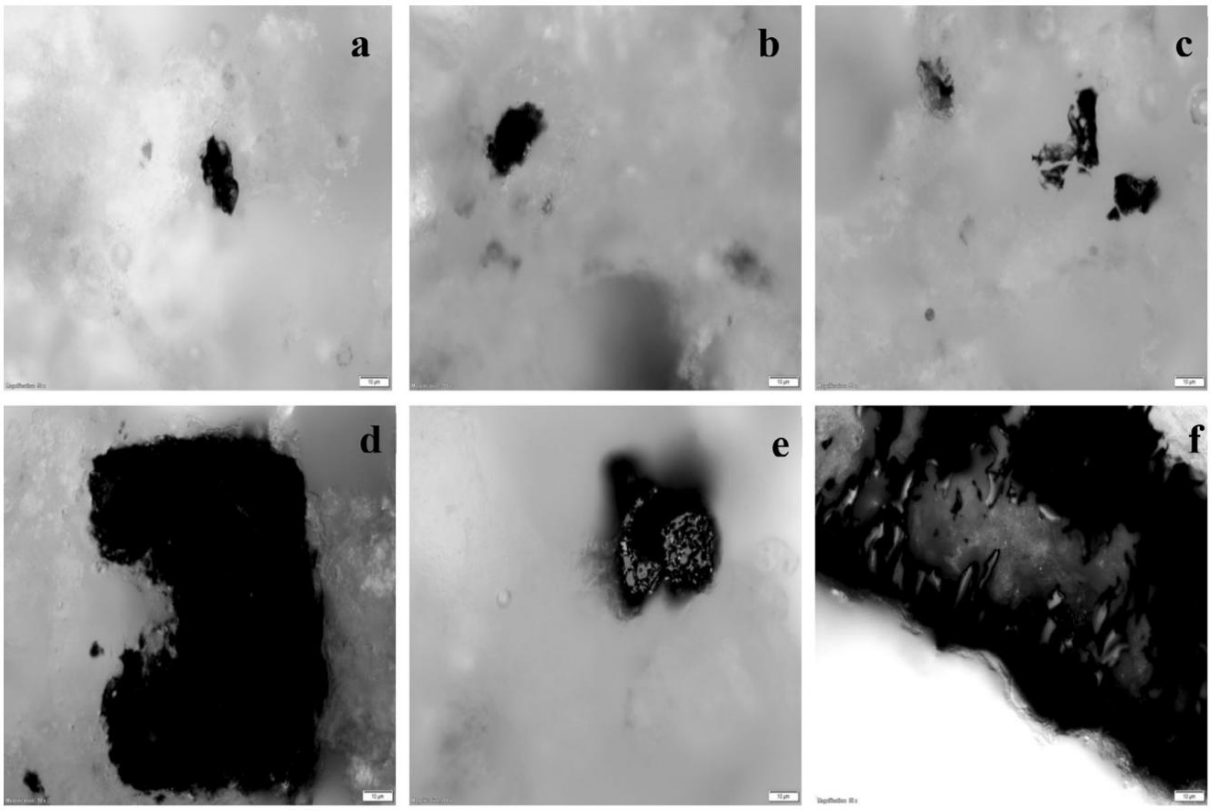

625
626
627 Figure 12 Micrographs and EDS spectra of “Gures” (Turkey) Economizer fly ash (SEM-EDS BSE
628 mode): A) global sample overview (×500); B) magnification of white square in “A” (×2000); C)
629 polished block overview and EDS marked morphotypes (×500); D) magnification of Z1 area in “C”
630 and EDS spectrum: irregular Ca-Si<<(Al-Mg) particle (×4000); E) magnification of Z2 area in “C” and
631 EDS spectrum: phosphosphere (×3000); F) magnification of Z3 area in “C” and EDS spectrum:
632 irregular CaO particle with Mg-Si-K (×4000); G) Ca-Si (Z6) and $CaCO_3$ sand (Z7) fragments, and Z6
633 EDS spectrum (polished block; ×2500); H) Z7 EDS spectrum in “G”; I) size-fraction <25 µm: Z1
634 particle and respective EDS showing high-peaks of P and Ca and minors of K and Mg (global
635 sample; ×5000); J) Z2 EDS spectra in “I” of a $CaCO_3$ fragment covered by KCl and Ca-sulfate; K) KCl
636 crystals (Z3 EDS spectrum) adsorbed at a particle surface (global sample; ×15000).
637
638

Figure 13 Rim mineralogy and evidence of particles ageing (micrographs A-C and G-I are polished blocks; bottom ash from "Gures", Turkey; SEM-EDS BSE mode): A) grain of $CaCO_3$ with a thick rim (×53); B) magnification of dashed square in "A": $CaCO_3$ (Z1), cryptic $CaCO_3$ (Z2), rim (Z3) (×150); C) magnification of dashed square in "A": (×500); D-F) EDS spectra Z1, Z2 and Z3 in "B"; G) magnification of dashed square in "C": cryptic $CaCO_3$ (×2500); H) $CaCO_3$ grain partially fragmented with a cryptic surface surrounded by a rim (×67); I) magnification of dashed square in "K": rim with Ca and Ca-P bands (×750); J) "old" grain with cryptic $CaCO_3$ with detaching rim (×128); K) magnification of dashed square in "C": cryptic $CaCO_3$ (×900).

Figure 14 Rim formation (polished blocks of bottom ash from "Gures", Turkey; SEM-EDS BSE mode): A) $CaCO_3$ sand (Ca) with an early stage rim formation (r) (×100); B) magnification of white square in "A" and EDS (Z8) of the $CaCO_3$ (×2000); C) Z7 EDS spectrum in "B": rim composition; D) early-stage formation Ca-P rim (Z3 EDS spectrum) at $CaCO_3$ surface (×15000); E-F) variation of rim composition as it gets thicker (×15000); G) fragment of a detached rim (×1500); H) magnification of dashed square in "G": hydroxyapatite crystals and respective EDS (Z6) spectrum (×10000).

Figure 15 P-inorganic amorphous and phosphospheres in Gures Economizer (FAECO) and Cyclone (FACYC) fly ash samples (polished blocks; SEM-EDS BSE mode): A) overview of FACYC (×100); B) overview of FAECO (×1000); C) Ca- (Z7) and P-rich (Z8) inorganic amorphous from laying hens excreta and Z7 EDS spectrum (FACYC; ×750); D) EDS spectra Z8 in "C"; E) structureless phosphospheres will hole (FAECO; ×3000); F) dense and structureless magnesia-phosphosphere (FACYC; ×4000); G) Mg-K-phosphosphere with pomegranate structure and Mg-rich matrix, and Z1 EDS spectrum (FAECO; ×10000); H) EDS spectra Z2 in "G"; I) phosphosphere with pomegranate structure and Mg-K-rich matrix, and Z11 EDS spectrum (FACYC; ×1500); J) phosphosphere with pomegranate structure and Mg-K-rich matrix, and Z6 EDS spectrum (FACYC; ×1500); K) magnification of pomegranate structure in "J", and Z7 EDS spectrum (×5000).

Organic matter morphotypes identification by optical microscopy

The petrographic study of the ash samples aims the evaluation the structural and textural composition. The research of microtexture and microstructure highlight some aspects of theoretical and practical interest regarding the aviary waste combustion process, as evolution and efficiency, as well as on characteristics of resulting ash, respectively: development of the process and phenomena that take place; details on combustion parameters, combustion plant optimisation and thermodynamic parameters; origin of biomass; type and size of the porosity [47].
In this study, optical microscopy was used to identify the residual carbon resulting from incomplete rice husk combustion generates interesting morphological aspects complementary to those identified by electron microscopy (SEM analysis revealed by Figures 6A and B, 7A, and B, 9B and 11F, G).
The analysis of residual carbon originating from biomass - rice husks (used as aviary bed at Campoaves) is observed mostly in BA than FA in the studied samples. Some textural aspects of partially burned carbon, sporadically identified, corresponds to low carbon contents below 10%. Residual carbon (biochar) appears in the photomicrographs of Figure 16 (A-F), in which the char derived from rice straw can be easily identified by its elongated and porous appearance.

Figure 16 Photomicrographs of rice husk biochar (Campoaves samples), Reflected Light, oil immersion, 500x.

The optical appearance of carbon particles is exclusively isotropic and intensely porous.
The existence of biochar porosity may facilitate the condensation in these pores of certain substances removed during devolatilisation. In the case of using ash as a soil supplement, they may be released sequentially in contact with rainwater and depending on the soil pH.
In Güres ash samples, biomass is sporadic and difficult to evaluate from a morphological point of view. The optical aspect of carbon particles is exclusively isotropic, dense, and free of porosity. However, some char particles can be identified with specific biomass textures but with an uncertain aspect regarding the origin, in Figure 17. Although at Güres, a vegetable bed was not used for poultry farms, the source of these microscopically identified char fragments is explained by the presence of plant remains leftover from bird feed.

Figure 17. Photomicrographs of residual carbon of biomass origin from fluidised combustion of aviary waste (Güres samples), Reflected Light, oil immersion, 500x.

The analysis of the ash samples by both SEM and optical microscopy highlights similar morphological aspects, easy to identify. The micrographs taken under the optical microscope are like those identified by SEM (magnification 300X) in which fragments of biomass char (residual carbon) appear with porous structures. In addition to the optical, morphological analysis by which the presence of carbon is identified, EDS analysis confirms this aspect. The inner layer of rice husks was spectrally identified (see SEM-EDS results).

Trace elements evaluation: EU regulatory framework for fertilisers application

Based on the chemical characterisation, rice husk poultry litter ash and laying hens manure (with $CaCO_3$ sand) ash are potential direct fertilisers according to the EU regulation 209/1009 of the European Parliament of 5 June 2019 [48]. The latter defines a fertiliser as follows: "shall be an EU fertilising product the function of which is to provide nutrients". Therefore, thanks to macronutrients such as P and K, Campoaves and Güres ash samples are among the materials candidate to show good bioavailability in pot and field tests. In addition, these incinerated ashes are free of pathogenic substances [49].

Trace elements such as Cu, Zn, Rb, Ba, Sr were quantified using digestion and lithium tetraborate/metaborate fusion (Table 3), including REE+Y and seventh-period elements such as uranium. Campoaves and Güres samples have similar concentrations of Ni, Co, W, Se and Pb. The REE+Y, U and Th concentrations are relatively higher in Campoaves samples. They may be due to the rice husk as poultry litter taken from paddy fields that typically contains trace elements such as rare earth elements [45]. However, in both cases, the concentrations of REE+Y, U and Th are low. Results are, therefore, promising for the use of ashes as fertilisers since the trace element concentrations are lower than that reported in the literature for phosphate rocks (see Table 5).

At this point, it could be interesting to evaluate if the quantity of the trace elements and minor elements, specifically Zn and Cu, comply or not with EU regulation. This legislative act reports that for particular recovered wastes, such as struvite, biochar and ash-based products (like in the present case), within the meaning of Directive 2008/98/EC [50], market demand for the use of these ashes as a fertilising product is possible as long as specific requirements are fulfilled. Article 4 of this document reports that the product should meet the criteria set out in Annex I for the

function category as a significant obstacle rather than Annex II providing for the component category and Annex III related to the labelling requirements.

There are specific limits for contaminants (Hg, Cr(VI), Ni, Pb, As, Cd, Cu, Zn) based on the function categories differentiated by application purpose: fertilisers for nutrient uptake for the plants, liming material, soil-improving, growing medium for inhibition of urease and nitrification/denitrification inhibitor, plant bio-stimulation. Based on the amount of the macronutrients present on Campoaves and Güres samples, all the samples have nutrients in oxide form such as P_2O_5 (3 %), K_2O (3 %), MgO (3 %), CaO (1.5 %), SO_3 (1.5 %) and NaO (1 %), higher than 3, 3, 3, 1.5, 1.5 and 1 %, respectively, required for inorganic macronutrient fertilizers. Under the EU regulation, this material shall provide plants or mushrooms with at least two primary nutrients among P, K, N and at least two secondary nutrients among Ca, Mg, S, Na.

Regarding this function category, all the samples comply with the limits set for Cd (values under the limit of 6 ppm in case of P_2O_5>5 %), Cr(VI) (in the present work, Total measured Cr is less than 1 ppm), Hg (lower than 1ppm), Ni (under the limit of 100 ppm), Pb (<120 ppm), As (<40 ppm), Cu (<600 ppm).

Zinc, however, is an exception since FAECO-CA (2516 ppm), FACYC-CA (2221 ppm), and FAECO-GU (2356 ppm) samples do not respect the limits (1500 ppm) for this category. The reason relies on the oxidation in lighter particles corroborating the data shown in the elemental analysis in Table 1 where the concentration of minor elements increased in the post-combustion section. Nevertheless, beneficiation of the ashes via excluding some ashes or its dilution overcome the problem if a direct application as fertilisers is considered.

Table 4. Comparison of selected trace elements concentration (ppm) from ICP-MS data of Table 3 with data reported for phosphate rock [51].

Conclusions

The comparative characterisation study between two sub-categories of incinerated aviary by-products has been done for the first time yield the following results

- P in the ash is speciated in different minerals: the Güres ash is dominated by hydroxyapatite mineral form, and the Campoaves ash contains, in addition to hydroxyapatite, other P-bearing minerals, such as K-struvite, $Ca_3(PO_4)_2$ and NaH_2PO_4, as the main phases.

Ca-rich Güres ash and Si-rich Campoaves ash are characterized by two different mineral assemblages resulting from two distinct combustion systems. In the Güres plant, the use of calcite as a bed particle for the fluidised combustion explains the formation of Ca phases. The typology of the flock (poultry excreta, spilled feed and feathers are retained by rice husk, rich in SiO_2, forming poultry litter) also differs in the two sites.

- These two ashes display features corresponding to the K type for Campoaves and the C/CK type for Güres from Vassilev's classification.

The other difference concerns the trace elements contents, linked to the geo-location of the fuel material: the higher REE, Th concentrations of Campoaves samples are due to their presence in open area agricultural fields.

- Finally, both samples showed that under the EU regulatory framework, they could readily comply with the limitations set for the functional category of inorganic macronutrient fertilisers application, which facilitates the way to push for marketing these ash residuals as nutrient providers for plants.

Declarations

Funding

This research was under the scope of the Program ERA-MIN2 of the European Commission, Project DEASPHOR entitled "Design of a product for substitution of phosphate rocks" and funded by FCT (Portugal; Ref. ERA-MIN/0002/2017) - UEFISCDI 48/2018 - CUP D81I18000190002.

Conflicts of interests

All authors certify that they have no affiliations with or involvement in any organisation or entity with any financial or non-financial interest in the subject matter or materials discussed in this manuscript.

Data availability

All data generated or analysed during this study are included in this published article (and its supplementary information files).

References

1. Hä Ggströ, G., Fü Rsatz, K., Kuba, M., Skoglund, N., Hman, M.Ö̈: Fate of Phosphorus in Fluidized Bed Cocombustion of Chicken Litter with Wheat Straw and Bark Residues. (2020). https://doi.org/10.1021/acs.energyfuels.9b03652
2. Luyckx, L., de Leeuw, G.H.J., Van Caneghem, J.: Characterisation of Poultry Litter Ash in View of Its Valorisation. Waste and Biomass Valorisation. 1, 3 (2019). https://doi.org/10.1007/s12649-019-00750-6
3. Bindraban, P.S., Dimkpa, C., Nagarajan, L., Roy, A., Rabbinge, R.: Revisiting fertilisers and fertilisation strategies for improved nutrient uptake by plants. Biol. Fertil. Soils. 51, 897–911 (2015). https://doi.org/10.1007/s00374-015-1039-7
4. Geissler, B., Hermann, L., Mew, M.C., Steiner, G.: Striving toward a circular economy for phosphorus: The role of phosphate rock mining. Minerals. 8, (2018). https://doi.org/10.3390/min8090395
5. European Commission: 20 critical raw materials - major challenge for EU industry. (2014)
6. Smol, M., Preisner, M., Bianchini, A., Rossi, J., Hermann, L., Schaaf, T., Kruopienė, J., Pamakštys, K., Klavins, M., Ozola-Davidane, R., Kalnina, D., Strade, E., Voronova, V., Pachel, K., Yang, X., Steenari, B.-M., Svanström, M.: Strategies for Sustainable and Circular Management of Phosphorus in the Baltic Sea Region: The Holistic Approach of the InPhos Project. Sustainability. 12, 2567 (2020). https://doi.org/10.3390/su12062567
7. Tirado, R., Allsopp, M.: Phosphorus in agriculture Problems and solutions. Greenpeace Res. Lab. Tech. Rep. 3–30 (2012)

8. Karunanithi, R., Szogi, A.A., Bolan, N., Naidu, R., Loganathan, P., Hunt, P.G., Vanotti, M.B., Saint, C.P., YongSik, O., Krishnamoorthy, S.: Chapter three - phosphorus recovery and reuse from waste streams. Adv. Agron. 131, 173–250 (2015)
9. van Dijk, K.C., Lesschen, J.P., Oenema, O.: Phosphorus flows and balances of the European Union Member States. Sci. Total Environ. 542, 1078–1093 (2016). https://doi.org/https://doi.org/10.1016/j.scitotenv.2015.08.048
10. A, N.B., B, A.S., A, B.S., A, T.C.: The management of phosphorus in poultry litter. World. 317–320 (2010)
11. Patterson, P.H., Moore Jr, P.A., Angel, R.: Phosphorus and poultry nutrition. Phosphorus Agric. Environ. 46, 635–682 (2005)
12. Kanani, F., Heidari, M.D., Gilroyed, B.H., Pelletier, N.: Waste valorisation technology options for the egg and broiler industries: A review and recommendations, (2020)
13. Florin, N.H., Maddocks, A.R., Wood, S., Harris, A.T.: High-temperature thermal destruction of poultry derived wastes for energy recovery in Australia. Waste Manag. 29, 1399–1408 (2009). https://doi.org/10.1016/j.wasman.2008.10.002
14. Ashworth, A.J., Chastain, J.P., Moore, P.A.: Nutrient Characteristics of Poultry Manure and Litter. 63–87 (2020). https://doi.org/10.2134/asaspecpub67.c5
15. Cavalaglio, G., Coccia, V., Cotana, F., Gelosia, M., Nicolini, A., Petrozzi, A.: Energy from poultry waste: An Aspen Plus-based approach to the thermo-chemical processes. Waste Manag. 73, 496–503 (2018). https://doi.org/10.1016/j.wasman.2017.05.037
16. Bolan, N.S., Szogi, A.A., Chuasavathi, T., Seshadri, B., Rothrock, M.J., Panneerselvam, P.: Uses and management of poultry litter. Worlds. Poult. Sci. J. 66, 673–698 (2010). https://doi.org/10.1017/S0043933910000656
17. HE, Z., PAGLIARI, P.H., WALDRIP, H.M.: Applied and Environmental Chemistry of Animal Manure: A Review. Pedosphere. 26, 779–816 (2016). https://doi.org/https://doi.org/10.1016/S1002-0160(15)60087-X
18. Hakan Bayraktar, Ö., Baki Unal, H., Cengiz Akdeniz, R., Alkan, I.: Evaluation possibilities of chicken manure in Turkey. Agric. Eng. 19, 5–14 (2015). https://doi.org/10.14654/ir.2015.154.116
19. Li, B., Boiarkina, I., Yu, W., Huang, H.M., Munir, T., Wang, G.Q., Young, B.R.: Phosphorous recovery through struvite crystallisation: Challenges for future design, (2019)
20. Vanotti, M.B., García-González, M.C., Szögi, A.A., Harrison, J.H., Smith, W.B., Moral, R.:

Removing and Recovering Nitrogen and Phosphorus from Animal Manure. Presented at the January 9 (2020)

21. Häggström, G., Engineering, E.: Experimental studies of ash transformation processes in thermochemical conversion of P-rich biomass and sludge. Presented at the

22. Huang, Y., Dong, H., Shang, B., Xin, H., Zhu, Z.: Characterisation of animal manure and cornstalk ashes as affected by incineration temperature. Appl. Energy. 88, 947–952 (2011). https://doi.org/10.1016/j.apenergy.2010.08.011

23. Vassilev, S. V., Baxter, D., Vassileva, C.G.: An overview of the behaviour of biomass during combustion: Part II. Ash fusion and ash formation mechanisms of biomass types. Fuel. 117, 152–183 (2014). https://doi.org/10.1016/J.FUEL.2013.09.024

24. Santos Dalólio, F., da Silva, J.N., Carneiro de Oliveira, A.C., Ferreira Tinôco, I. de F., Christiam Barbosa, R., Resende, M. de O., Teixeira Albino, L.F., Teixeira Coelho, S.: Poultry litter as biomass energy: A review and future perspectives, (2017)

25. Mierzwa-Hersztek, M., Gondek, K., Jewiarz, M., Dziedzic, K.: Assessment of energy parameters of biomass and biochars, leachability of heavy metals and phytotoxicity of their ashes. J. Mater. Cycles Waste Manag. 21, 786–800 (2019). https://doi.org/10.1007/s10163-019-00832-6

26. Leng, L., Bogush, A.A., Roy, A., Stegemann, J.A.: Characterisation of ashes from waste biomass power plants and phosphorus recovery. Sci. Total Environ. 690, 573–583 (2019). https://doi.org/10.1016/j.scitotenv.2019.06.312

27. European Commission: Directive 2000/76/EC of the European Parliament and of the Council of 4 December 2000 on the Incineration of Waste. Off. J. Eur. Communities. L 269, 1–15 (2000). https://doi.org/2004R0726 - v.7 of 05.06.2013

28. Fahimi, A., Bilo, F., Assi, A., Dalipi, R., Federici, S., Guedes, A., Valentim, B., Olgun, H., Ye, G., Bialecka, B., Fiameni, L., Borgese, L., Cathelineau, M., Boiron, M.-C., Predeanu, G., Bontempi, E.: Poultry litter ash characterisation and recovery. Waste Manag. 111, 10–21 (2020). https://doi.org/10.1016/j.wasman.2020.05.010

29. En, D.S.: Dansk standard Fast biobrændsel – Bestemmelse af partikelstørrelsesfordeling – Del 2 : Sigtemetode med vibrerende sigter på 3 , 15 mm og derunder Solid biofuels – Determination of particle size distribution – Part 2 : Vibrating screen method using. (2015)

30. ISO 11722:2013: Solid mineral fuels — Hard coal — Determination of moisture in the general analysis test sample by drying in nitrogen. 2013, (2013)

31. ISO 1171:2010: Solid mineral fuels — Determination of ash. 2010, (2010)
32. ISO_10993-12: Solid mineral fuels — Determination of volatile matter. 61010-1 © Iec2001. 2003, 13 (2021)
33. Romanian Standard Association: ISO 622:1981(en), Solid mineral fuels — Determination of phorphorus content — Reduced molybdophosphate photometric method, https://www.iso.org/obp/ui/#iso:std:iso:622:ed-1:v1:en
34. Ingamells, C.O.: Lithium metaborate flux in silicate analysis. Anal. Chim. Acta. 52, 323–334 (1970). https://doi.org/https://doi.org/10.1016/S0003-2670(01)80963-6
35. ISO 7404-2: Methods for the petrographic analysis of coals — Part 2: Methods of preparing coal samples, (2009)
36. Fuertes, A.B., National, S., Marban, G., National, S., Rubiera, F., National, S.: Kinetics of Thermal-Decomposition of Limestone Particles in A Fluidised-Bed Reactor. (1993)
37. Fiameni, L., Assi, A., Fahimi, A., Valentim, B., Moreira, K., Predeanu, G., Slăvescu, V., Vasile, B., Nicoară, A.I., Borgese, L., Boniardi, G., Turolla, A., Canziani, R., Bontempi, E.: Simultaneous amorphous silica and phosphorus recovery from rice husk poultry litter ash. RSC Adv. 11, 8927–8939 (2021). https://doi.org/10.1039/d0ra10120f
38. Bogush, A.A., Stegemann, J.A., Williams, R., Wood, I.G.: Element speciation in UK biomass power plant residues based on composition, mineralogy, microstructure and leaching. Fuel. 211, 712–725 (2018). https://doi.org/10.1016/j.fuel.2017.09.103
39. Zafar, Z.I., Anwar, M.M., Pritchard, D.W.: Optimisation of thermal beneficiation of a low grade dolomitic phosphate rock. Int. J. Miner. Process. 43, 123–131 (1995). https://doi.org/https://doi.org/10.1016/0301-7516(94)00043-Y
40. Sınırkaya, M., Özer, A.K., Gülaboglu, M.S.: Investigation of the changes of P2O5 content of phosphate rock during simultaneous calcination/sulfation. Powder Technol. 211, 72–76 (2011). https://doi.org/https://doi.org/10.1016/j.powtec.2011.03.036
41. Vassilev, S., Baxter, D., Andersen, L., Vassileva, C., Morgan, T.: An overview of the organic and inorganic phase composition of biomass. Fuel. 94, 1–33 (2011). https://doi.org/10.1016/j.fuel.2011.09.030
42. Gumisiriza, R., Hawumba, J.F., Okure, M., Hensel, O.: Biomass waste-to-energy valorisation technologies: a review case for banana processing in Uganda. Biotechnol. Biofuels. 10, 11 (2017). https://doi.org/10.1186/s13068-016-0689-5
43. Alsaffar, M.S., Jaafar, M.S., Kabir, N.A., Ahmad, N.: Distribution of 226 Ra, 232 Th, and 40 K

in rice plant components and physico-chemical effects of soil on their transportation to grains . J. Radiat. Res. Appl. Sci. 8, 300–310 (2015). https://doi.org/10.1016/j.jrras.2015.04.002

44. Zhou, W., Han, G., Liu, M., Song, C., Li, X.: Geochemical distribution characteristics of rare earth elements in different soil profiles in Mun River Basin, Northeast Thailand. Sustain. 12, (2020). https://doi.org/10.3390/su12020457

45. Chen, H., Chen, Z., Chen, Z., Ma, Q., Zhang, Q.: Rare earth elements in paddy fields from eroded granite hilly land in a southern China watershed. PLoS One. 14, e0222330 (2019)

46. Tsumura, A., Yamasaki, S.: Behavior of uranium, thorium, and lanthanoids in paddy fields. Radioisot. 42, 265–272 (1993)

47. Predeanu, G., Popescu, L., Abagiu, T., Panaitescu, C., Valentim, B., Guedes, A.: Characterisation of bottom ash of Pliocene lignite as ceramic composites raw material by petrographic, SEM/EDS and Raman microspectroscopical methods. Int. J. Coal Geol. 168, (2016). https://doi.org/10.1016/j.coal.2016.08.004

48. The European Parliament and the Council of the European Union: Regulation (EU) 2019/1009 of the European Parliament and of the Council of 5 June 2019 laying down rules on the making available on the market of EU fertilising products and amending Regulation (EC) No 1069/2009 and (EC) No 1107/2009 and repealing Regulat. (2019)

49. Luyckx, L., De Leeuw, G.H.J., Caneghem, J. Van: Characterisation of poultry litter ash in view of its valorisation. Loizidou and Moustakas (2018)

50. European Council: Directive 2008/98/CE of the European Parliament and of the Council of 19 November 2008 on waste and repealing certain Directives. Off. J. Eur. Union. L312, 1–59 (2008)

51. Chen, M., Graedel, T.E.: The potential for mining trace elements from phosphate rock. J. Clean. Prod. 91, 337–346 (2015). https://doi.org/10.1016/j.jclepro.2014.12.042